3024

CHAPTER 36

ADSORPTION HYSTERESIS

D. H. Everett

DEPARTMENT OF PHYSICAL CHEMISTRY
SCHOOL OF CHEMISTRY
UNIVERSITY OF BRISTOL
BRISTOL, ENGLAND

36-1. Definition of Hysteresis 1055
36-2. Survey of Adsorption Hysteresis 1058
A. Historical 1058
B. Classification of Adsorption Hysteresis 1058
C. Scanning Curves 1067
36-3. Theories of Adsorption Hysteresis 1072
A. Some General Thermodynamic Considerations 1072
B. The Domain Concept 1073
C. Generalized Phase-Change Theories 1075
D. Capillary Condensation Theories 1076
E. Low-Temperature Hysteresis 1089
F. Low-Pressure Hysteresis 1089
36-4. Experimental Evidence for Capillary Condensation 1092
36-5. Domain Effects in Adsorption Hysteresis 1095
A. General Considerations 1095
B. The Independent-Domain Theory 1097
C. Interdependence of Domain Processes 1103
36-6. Summary 1110
References 1110

36-1. DEFINITION OF HYSTERESIS

A process is said to exhibit *hysteresis* if, when the direction of change of an independent variable x is reversed, a dependent variable Y fails to retrace the values through which it passed in the forward process; the dependent variable "lags behind" in its attempt to follow the changes in the independent variable (*1*); Fig. 36-1a. It is usually found that, if the independent variable oscillates between a lower bound x_l and an upper bound x_u, the dependent variable, when plotted against the independent variable, executes a closed loop; see Fig. 36-1b. We shall not be concerned in this account with the possible behavior in which the dependent variable drifts steadily; see Fig. 36-1c. In some systems the size of the hysteresis loop depends upon the speed with with the loop is traversed and, hence, upon the frequency of the oscillation of the independent variable. When experiments are carried out very slowly, the loop may degenerate into a line, and hysteresis may disappear; see Fig. 36-1d. Time-dependent hysteresis is caused by relaxation phenomena of a kind which lies outside the scope of the present discussion (*2*); we consider here only "permanent hysteresis."

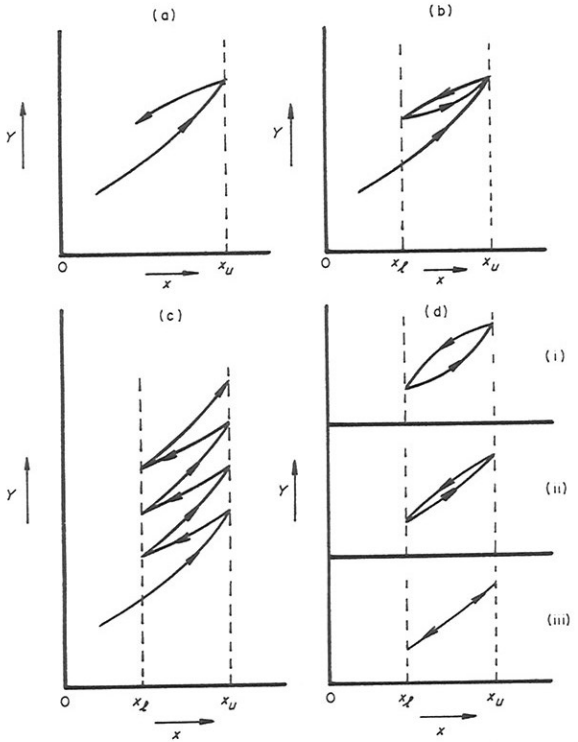

FIG. 36-1. (a) Reversal of path of system showing hysteresis. (b) Formation of closed loop by oscillation between x_u and x_l. (c) Drift as a result of oscillation between x_u and x_l. (d) Loop size dependent on frequency of oscillation: (i) → (iii) decreasing frequency.

Hysteresis may be observed over the whole range of physically attainable values of x or be confined to a limited range of values. In either case the loop corresponding to the maximum range of values of x over which hysteresis occurs is called the *boundary loop* or *main loop*; it consists of the *ascending boundary curve* (x increasing) and the *descending boundary curve* (x decreasing); see Fig. 36-2a, b. If an ascending path along the boundary curve is reversed before the limit of the loop is reached, then the system follows a path, called a *descending scanning curve*, across the loop; see Fig. 36-2c. Similarly, an *ascending scanning curve* may be traced, from the descending boundary curve; see Fig. 36-2d.† Later we shall examine in detail other paths that are available to the system within the boundary loop.

† Scanning curves that begin from a point on a boundary curve are sometimes called *primary* scanning curves (*3*).

In discussing the adsorption of a single gaseous component on a solid we shall choose as independent variable the partial pressure p of a gas in equilibrium with the adsorbed phase. The dependent variable may be the amount n^a of material adsorbed, a macroscopic physicalp roperty of the solid adsorbent such as its linear dimensions, a mechanical property, or an electrical

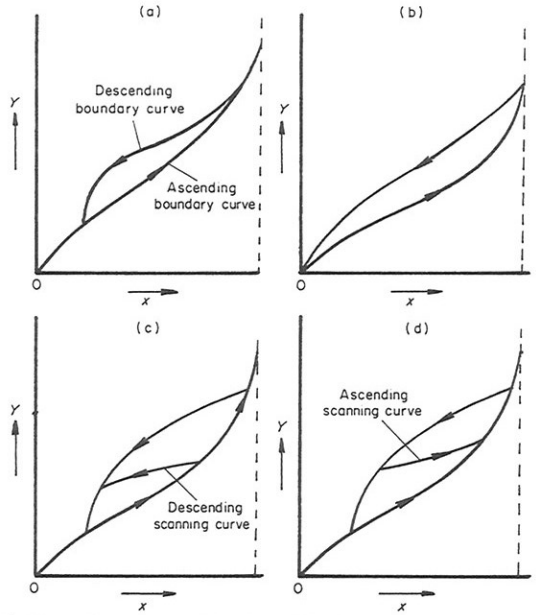

FIG. 36-2. Definition of terms used in describing hysteresis phenomena. See text for explanation.

property. In this chapter, however, we consider only the interdependence of the amount adsorbed and the partial pressure.

It is usually observed in an adsorption experiment that, when the gas pressure is changed, apparent adsorption equilibrium is set up in a period varying from a few minutes to a few hours, depending on the degree of subdivision of the solid, its porosity, the region of the isotherm under investigation and, in some instances, the characteristics of the apparatus. In physical adsorption the rate of attainment of equilibrium is generally supposed to be controlled by diffusion processes in the gas or in the adsorbed phase, or both. Once this state is reached, the properties of the system remain constant, within the precision of observation, for periods of time many powers of ten greater than the "half-time" of the initial process. If under these conditions

the system exhibits hysteresis, we presume that it is justifiable to regard the properties of the system as equilibrium values, even though, as we shall see later, they may correspond to states of metastable equilibrium. A further important experimental characteristic of adsorption hysteresis is that, within the limits of observation, all adsorption and desorption curves are smooth and show no discontinuities.

36-2. SURVEY OF ADSORPTION HYSTERESIS

A. Historical

Hysteresis in the adsorption of water on silica gel was first reported by van Bemmelen in 1897 (*4*), and his observations, together with Ewing's work (*1*) on magnetic hysteresis, were the only experimental data available to test the earlier attempts, made by Brillouin (*5*) and Duhem (*6*), to establish a general thermodynamic theory of hysteresis. Fourteen years later Zsigmondy (*7*) and Anderson (*8*), working in Zsigmondy's laboratory, provided the first reasonably accurate experimental data and proposed the first detailed theory of adsorption hysteresis. The status of the phenomenon of hysteresis in adsorption was, however, frequently challenged during the following thirty years. It was claimed, for example, that hysteresis arose from the presence of impurities on the surface or in the gas phase, from failure to allow sufficient time for equilibration, or from other shortcomings in experimental technique. Criticisms of this kind could with some justification be levelled at some of the early experimental work, but the very careful researches of Lambert and his co-workers (*9*) in the period 1928–36 provided strong evidence for the fundamental nature of the phenomenon. This view was, however, not universally accepted until a much larger body of experimental evidence had been built up by means of more modern techniques, although it may be commented that some of the later work did not always match the very high standard set by Lambert. Even in 1944 Cohan (*10*) hesitated to accept the reality of the phenomenon in the case of adsorption on certain charcoals. He comments: "The following results on charcoal are presented with reservations . . . ." Further extensive work on a wide variety of systems (*11*) has now established beyond reasonable doubt the reality, reproducibility, and fundamental characteristics of adsorption hysteresis.

B. Classification of Adsorption Hysteresis

Adsorption hysteresis can exhibit a wide variety of forms with many special characteristics. Despite these differences, however, adsorption hysteresis phenomena conform to certain broad generalizations, which they share with hysteresis phenomena in other fields of physical chemistry and physics. Some of these characteristics are described in outline in Section

36-2C and discussed in greater detail after the general theoretical basis of hysteresis has been established.

A convenient classification of adsorption hysteresis may be based on the pressure range over which the main boundary loop extends. An alternative and somewhat more detailed classification, which takes account also of the

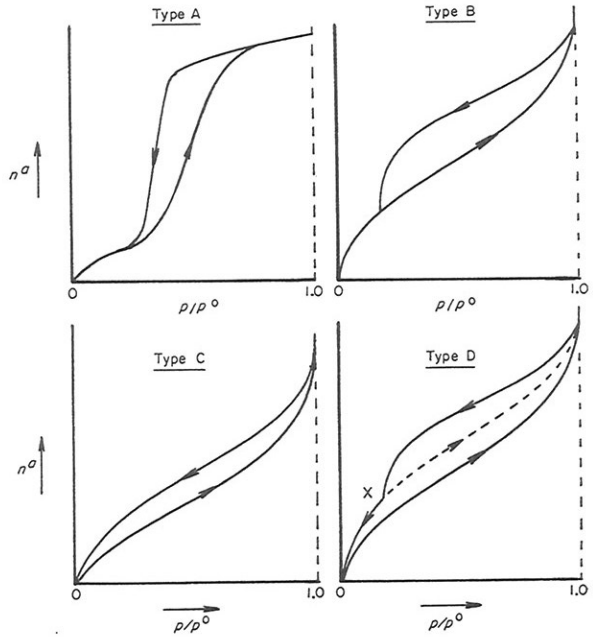

FIG. 36-3. Classification of adsorption hysteresis.

steepness of the adsorption and desorption branches, has been proposed by de Boer (*12*).

Some of the possibilities are shown schematically in Fig. 36-3 and compared with examples of experimental data in subsequent figures. A loop of type A is formed over a limited range of pressures; typical examples of systems that behave in this way are benzene adsorbed on silica gel (*8*) and on ferric oxide gel (*9*), noble gas plus porous glass around the triple-point temperature of the adsorbate (*13*), and nonpolar gas plus cracking catalyst (*14*); see Fig. 36-4. Hysteresis loops of type B extend from the saturation vapor pressure down to a well-defined closure point, which often seems to be more a characteristic of the vapor concerned than of the detailed structure of the adsorbent: the adsorption of nonpolar gases on porous carbons (*15*) and

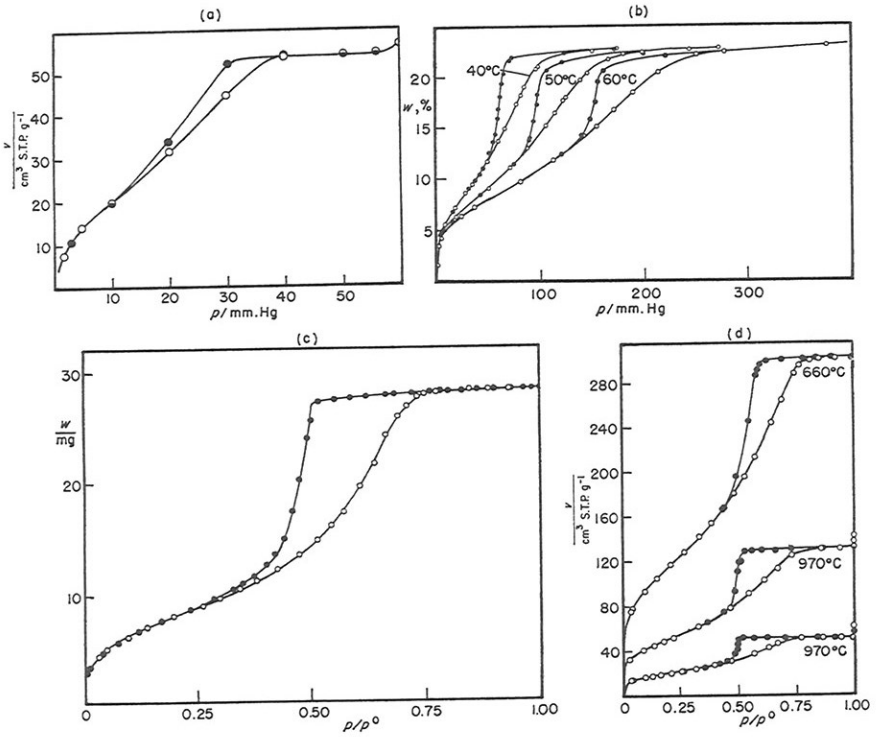

FIG. 36-4. Hysteresis loops of type A. (a) Benzene on silica gel at 15°C (*8*). (b) Benzene on ferric oxide gel at 40, 50, and 60°C. [Redrawn from (*9*) by permission of the Royal Society.] (c) Krypton on porous glass at 117.41°K (*13*); weight of sample, 61.60 mg. (d) Nitrogen on cracking catalyst sintered in vacuo for various times at the temperatures shown on the curves. [Redrawn from (*14*) by permission of Academic Press.]

of both polar and nonpolar gases on certain zeolitic materials (*16*) usually falls into this category; see Fig. 36-5a, b, c. Often the adsorption isotherm becomes effectively vertical at the saturation vapor pressure, and the position of the desorption curve may depend upon the maximum uptake reached at the saturation vapor pressure [(*15a*); see Fig. 36-5d]. In other cases, such as the adsorption of water on cellulosic or protein fibers (*17*) or of polar adsorbates on montmorillonite (*16*), the loop extends over the whole pressure range, type C; see Fig. 36-6a, b. A similar phenomenon occurs in the adsorption of ammonia on graphitized carbon black (*18*); see Fig. 36-6c. Finally, a loop, type D, may combine the general characteristics of types B and C. The desorption curve falls rapidly at a point characteristic of a type B loop, but

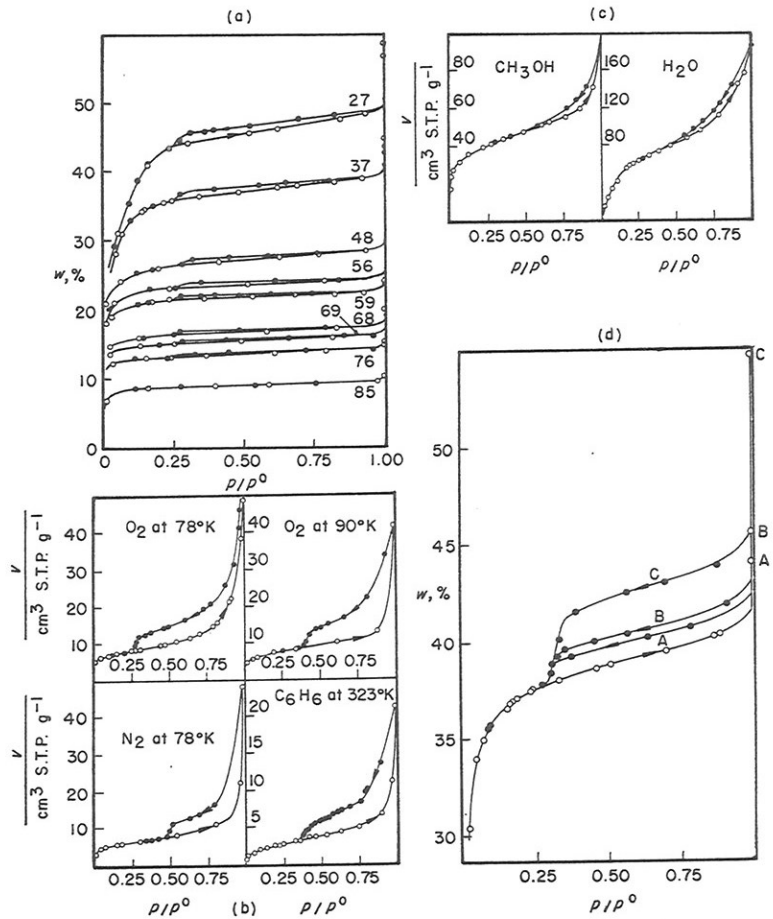

FIG. 36–5. Hysteresis loops of type B. (a) Benzene on a series of steam-activated anthracite coal charcoals at 25°C; figures give the "activation yield" (100 minus percentage of carbon removed in steam activation). [Redrawn from (*15b*) by permission of Society of Chemical Industry.] (b) Nonpolar sorbates on natural montmorillonite. [Redrawn from (*16*) by permission of Butterworth.] (c) Polar sorbates on tetramethylammonium montmorillonite. [Redrawn from (*16*) by permission of Butterworth.] (d) Benzene on activated coconut shell charcoal at 35°C (*15a*): desorption curves A, B, C commenced from points A, B, C on vertical section of isotherm.

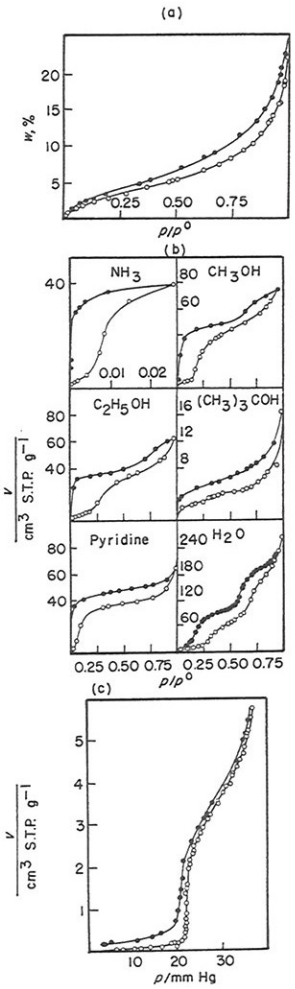

FIG. 36-6. Hysteresis loops of type C. (a) Water on soda-boiled cotton at 25°C. [Redrawn from (*17*) by permission of the Textile Institute.] (b) Polar sorbates on natural montmorillonite at 50°C. [Redrawn from (*16*) by permission of Butterworth.] (c) Ammonia on Sterling M.T. (3000) graphitized carbon black at −78°C. [Redrawn from (*18*) by permission of American Chemical Society.]

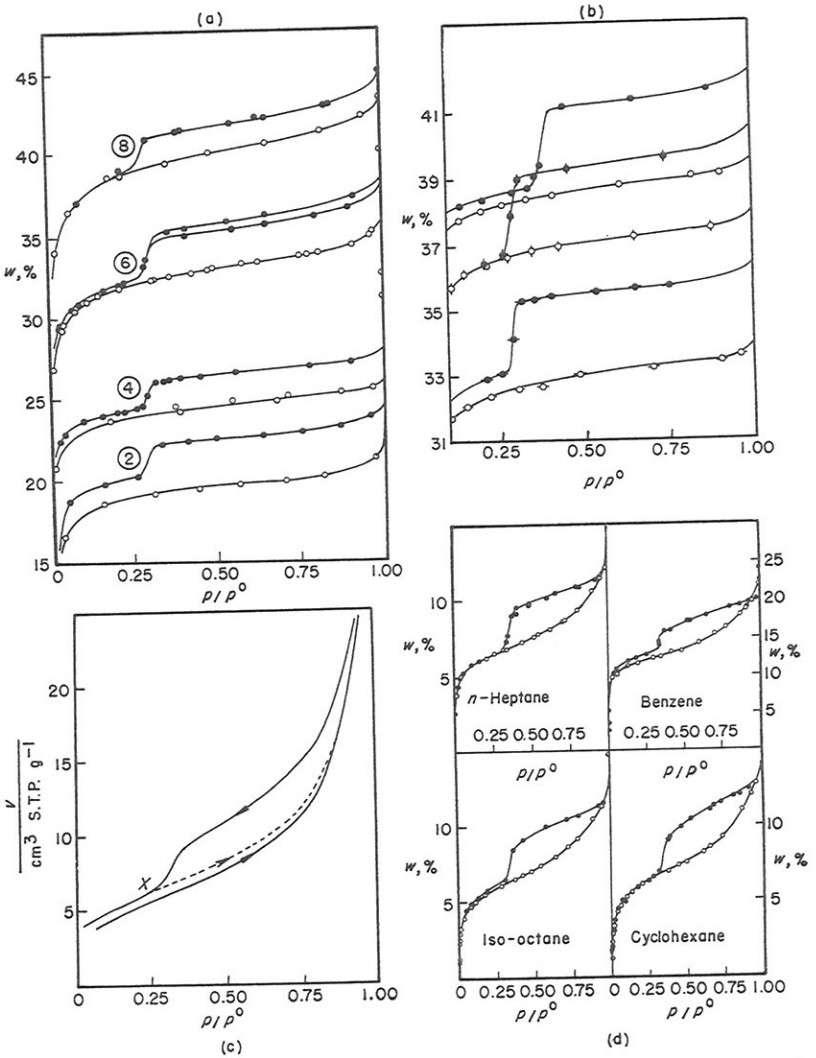

FIG. 36-7. Hysteresis loops of type D. (a) Benzene on a series of steam-activated coconut shell charcoals at 25°C, showing transition from type D to type B as activation proceeds (*15a*). Numbers refer to serial numbers of charcoals in Lemieux and Morrison, *Can. J. Res.*, **B25,** 440 (1947). (b) *n*-Hexane (O), benzene (Ọ), and cyclohexane (-O-) on unactivated polyvinylidene chloride char at 25°C, showing dependence of type of hysteresis on molecular size and shape (*19*). (c) Nitrogen on artificial graphite at 71°K. [Redrawn from (*11*) by permission of Butterworth.] (d) Hydrocarbons on methylammonium montmorillonite at 45°C. [Redrawn from (*20*) by permission of the Faraday Society.]

before it reaches the adsorption curve it turns away, to run nearly parallel to it, and rejoins it only at zero pressure. Examples of this behavior are found in the adsorption of vapors on certain carbons, both porous (*15,19*) and nominally nonporous (*11*), and on zeolitic materials (*20*); see Fig. 36-7a, b, c, d. In the case of a type D isotherm it is usually found that, if the desorption process is reversed at a point, such as X, below the sharp fall in the curve, then the system returns to the saturation pressure along the dotted scanning curve shown. A reproducible loop can then be traced out between X and the saturation vapor pressure; see Fig. 36-7c. In effect, the contribution of the type B loop to the overall phenomenon can be identified and studied separately. Only when the system is taken back to zero pressure is the lower adsorption curve recovered; in many cases exact reproduction of this curve can be achieved only after outgassing at an elevated temperature, and sometimes several days' "annealing" of the adsorbent may be required (*19*). A number of instances have been reported in which a system shows a type B loop but two or more steep portions on the desorption curve (*21,22,23*); see Fig. 36-8 and cf. also Fig. 36-6b.

Hysteresis phenomena are frequently temperature-dependent. Thus, hysteresis may develop as the temperature is lowered or as the temperature is raised, whereas in other cases the loop may first decrease in size with rising temperature, pass through a minimum size, and then increase again (*24*); see Fig. 36-9a, b, c, respectively. It has also been observed that certain systems which exhibit type B behavior at one temperature may show a type D loop at a higher temperature (*25*), while in at least one case a system which behaves reversibly at a higher temperature shows a type C loop at a lower temperature (*11*); see Fig. 36-9d. Loops of type A or B disappear also if the temperature is raised toward the bulk critical temperature of the adsorbate. Few data are available, but those of Dubinin and his co-workers (*26*) on the adsorption of CO_2 on silica gel (Fig. 36-10) suggest that the loop vanishes some 50C° below the critical temperature.

It has long been recognized that the detailed pore structure of the adsorbent plays an important role in determining the nature of the hysteresis loop. This may be illustrated by the change in the size and shape of the hysteresis loop, which is observed when a given vapor is adsorbed by a series of active charcoals whose pore structure is steadily modified by steam activation (*15*) or by a series of catalysts that have been subjected to successively more severe sintering conditions (*14*); see Figs. 36-5a and 4d. It may be noted, however, that although the size and shape of the loop depend on the pore structure, the relative pressure at which the loop closes depends only on the gas adsorbed and on the temperature.

Loop shapes are not always easy to compare visually, because the hysteresis phenomenon is often superimposed on a basic reversible adsorption. For

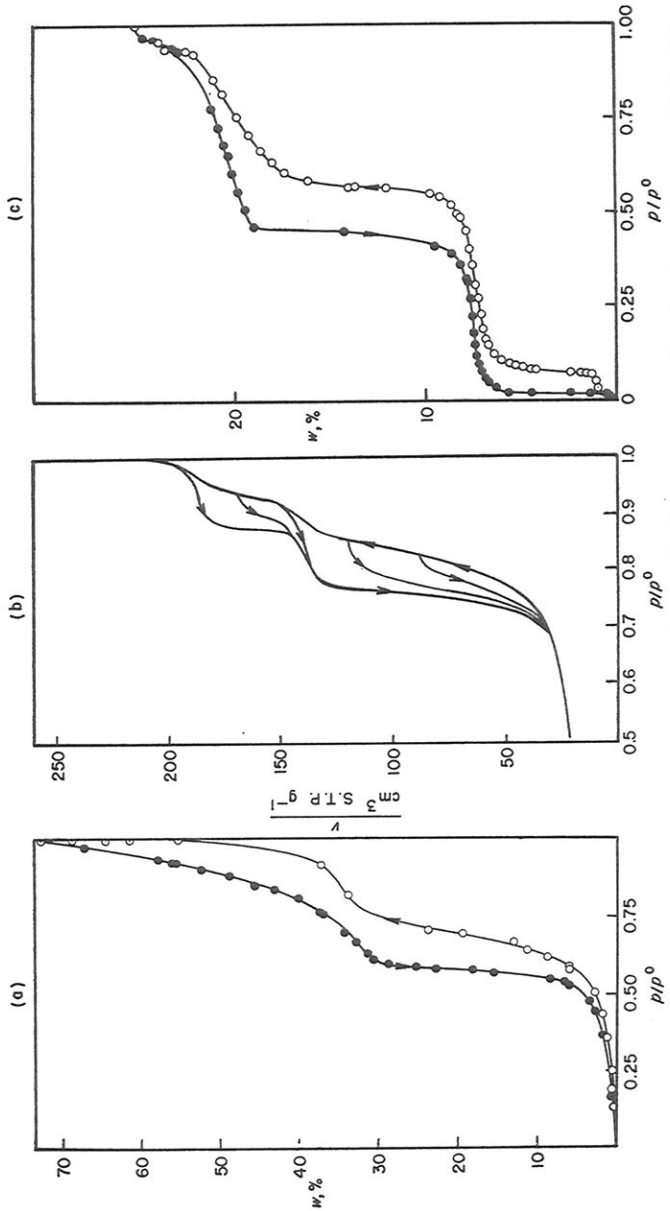

FIG. 36-8. Hysteresis loops of type D with two contributing loops. (a) Water on steam-activated soft-coal charcoal at 25°C (*15a*). (b) Nitrogen on porous glass treated with hydrofluoric acid. [Redrawn from (*22*) by permission of Société chimique de France.] (c) Water on sodium vermiculite at 25°C. [Redrawn from (*23*) by permission of Academic Press.]

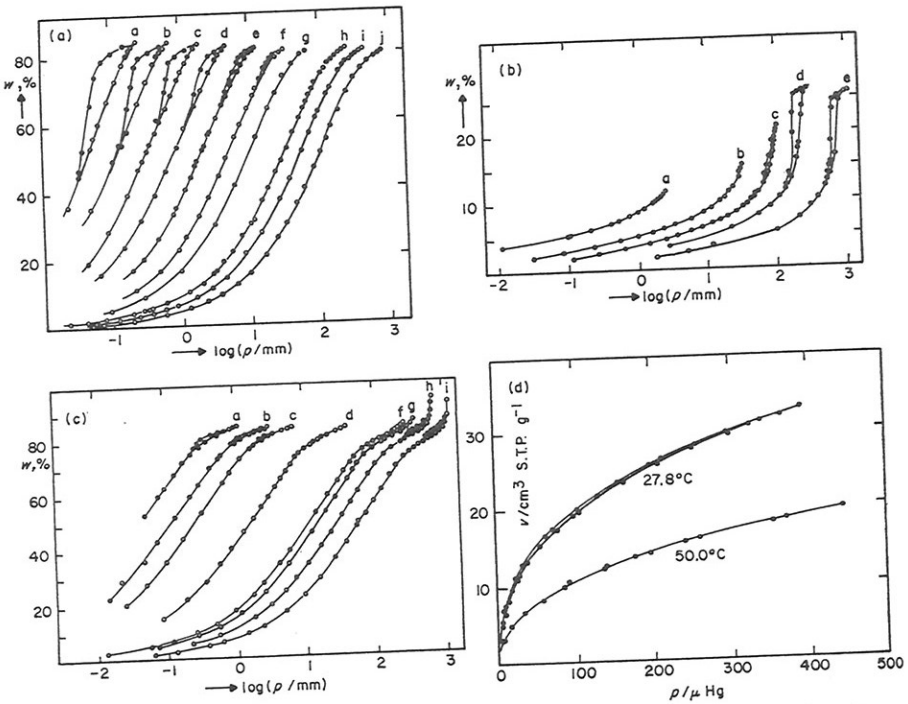

FIG. 36-9. Effect of temperature on adsorption hysteresis. (a) Carbon dioxide on activated coconut shell charcoal at a series of temperatures from (a) 130.4°K to (j) 196.3°K (*24*). (b) Nitrous oxide on porous glass at a series of temperatures from (a) 135.2°K to (e) 193.0°K (*24*). (c) Nitrous oxide on activated coconut shell charcoal at a series of temperatures from (a) 130.3°K to (i) 192.8°K (*24*). (d) Diethyl ether on charcoal activated with zinc chloride at 27.8 and 50.0°C (*11*). [(a) to (d) reproduced by permission of Butterworth.]

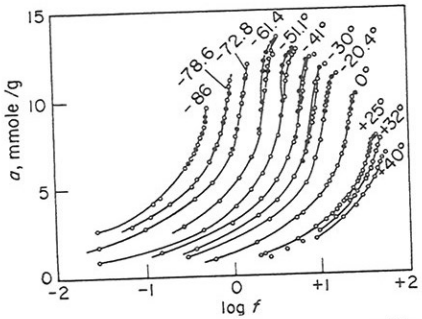

FIG. 36-10. Disappearance of hysteresis loop on approaching critical temperature: carbon dioxide on silica gel at a series of temperatures from −86 to +40°C. Amount adsorbed in millimoles per gram versus logarithm of fugacity of gas. [Reproduced from (*26*) by permission of Pergamon Press.]

comparative purposes it is often convenient to plot the vertical separation of the boundary curves (height of the loop) against pressure or against the chemical potential of the vapor measured by $\mathbf{R}T \ln p$; some examples of this type of graph are shown in Fig. 36-11a. Furthermore, in considering the thermodynamic aspects of hysteresis it is sometimes useful to consider the horizontal separation of the boundary curves (width of the loop), expressed in terms of

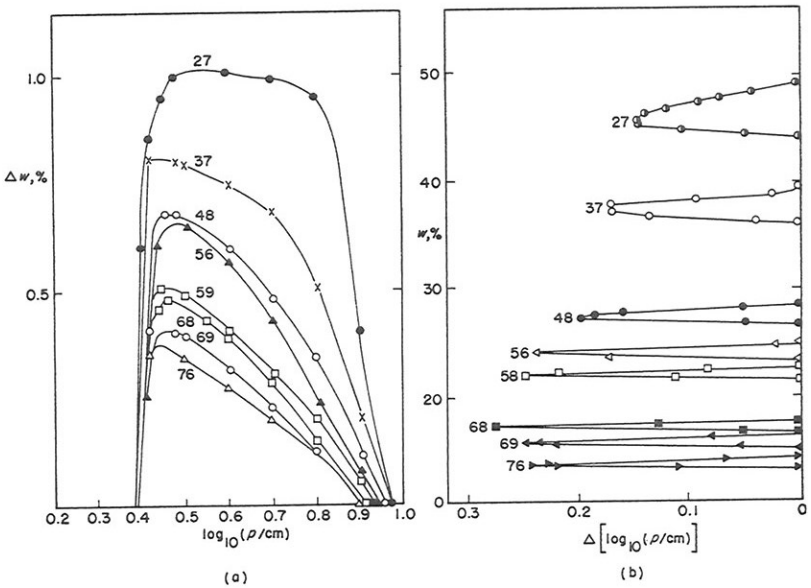

FIG. 36-11. Benzene on same series of steam-activated anthracite coal charcoals as in Fig. 36-5a (*15a*). (a) Height of loop (Δw/%) as a function of log [p/(cm Hg)]. (b) Width of loop in units of log [p/(cm Hg)] as a function of amount adsorbed.

$\mathbf{R}T \ln p$, as a function of the amount of material adsorbed. The width is a measure of the difference between the chemical potential of the adsorbate, when the same amount is present in the adsorbent, in the two extreme states represented by the boundary curves of the loop; see Fig. 36-11b.

C. Scanning Curves

Further important characteristics of hysteresis phenomena are revealed by a study of the scanning curves that can be followed across and within the main hysteresis loop (*27*). Some of the features of these curves are illustrated in Figs. 36-12, 36-13, 36-14, and 36-15. These are largely self-explanatory, but attention may be drawn to several interesting features. Typical sets of

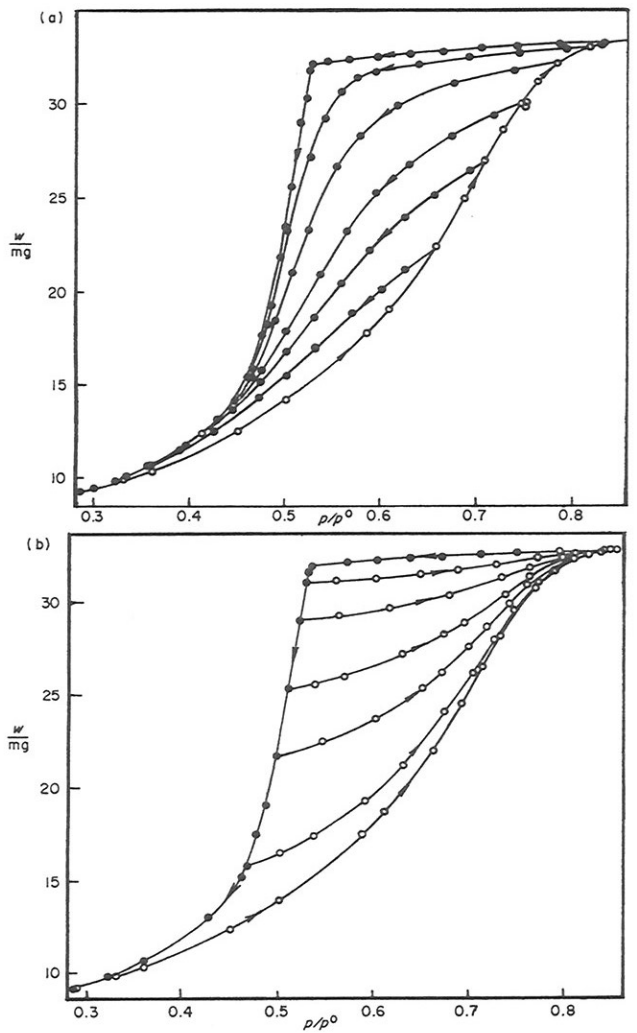

FIG. 36-12. Xenon on porous glass at 151.0°K (*13*). (a) Primary desorption scanning curves. (b) Primary adsorption scanning curves. Weight of sample, 61.60 mg.

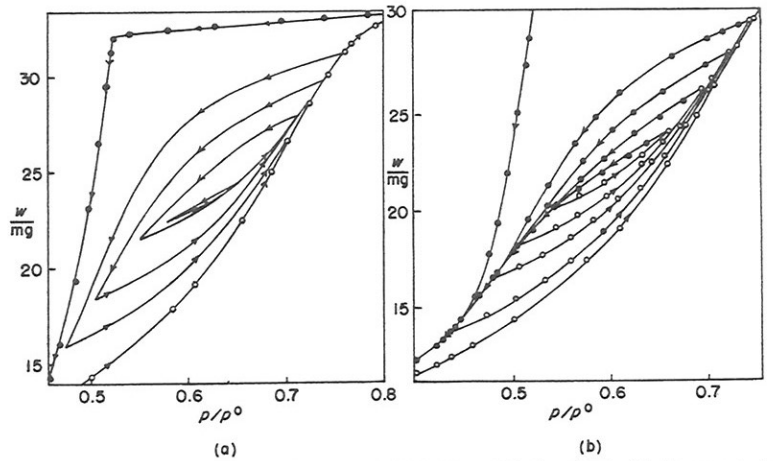

FIG. 36-13. Xenon on porous glass at 151.0°K (*13*). Spiral paths inside hysteresis loop ending with (a) adsorption process to boundary of loop and (b) desorption process to boundary of loop. Weight of sample, 61.60 mg.

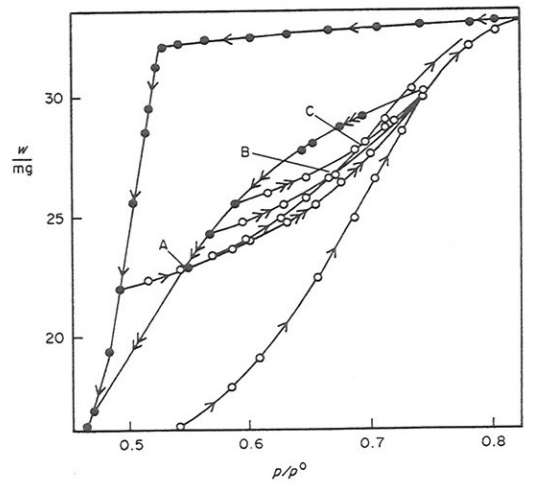

FIG. 36-14. Xenon on porous glass at 151.0°K (*13*): points A, B, C reached by different routes and showing different behavior on further adsorption. Weight of sample, 61.60 mg.

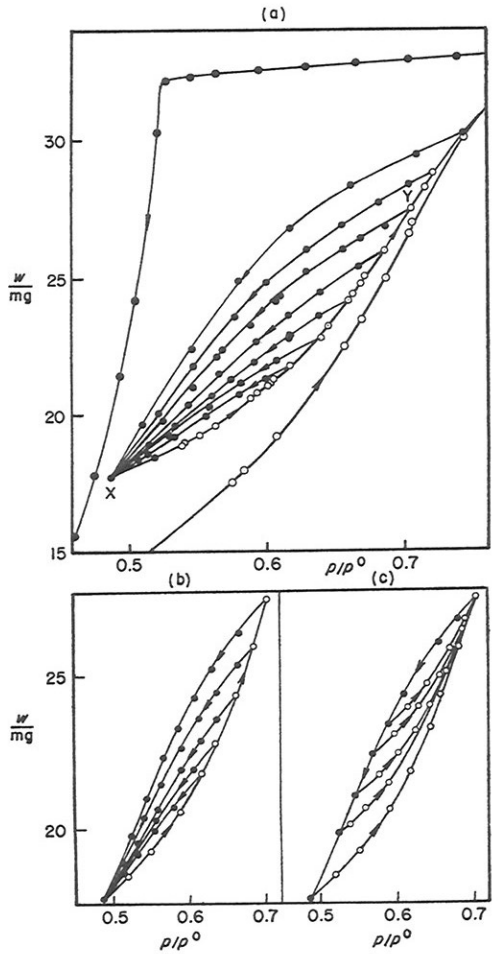

FIG. 36-15. Xenon on porous glass at 151.0°K (*13*). (a) Subsidiary loop inside main loop and desorption scanning curves. (b), (c) Adsorption and desorption scanning of loop between X and Y in (a). Weight of sample, 61.60 mg.

ascending and descending scanning curves (*13*) are shown in Fig. 36-12. Figure 36-13 shows how, by making a series of reversals at converging values of x_u and x_l, a spiral path can be traced. Return to the boundary loop from the center of the spiral by an ascending process is made by a path that passes through the set of upper reversal points of the spiral; see Fig. 36-13a.

Conversely, a descending process from the center passes through the set of lower reversal points; see Fig. 36-13b. Figure 36-14 illustrates the way in which it is possible to reach a given point within the loop by different routes, and that the path followed away from this point is dependent on the previous history of the system. A subsidiary loop within the main loop can be scanned in just the same way as the main loop, and this procedure can be carried out in several successive steps; see Fig. 36-15a, b, c. In studying the quantitative aspects of hysteresis phenomena it is convenient to compare the shapes and sizes of loops between the same upper and lower bounds but at different levels in the loop; see Fig. 36-16.

The existence and characteristics of the scanning behavior of a system showing hysteresis are important factors, which must be taken into account in developing a theory of the phenomenon. We shall therefore postpone discussion of Figs. 36-12 to 36-16 until we have considered the theory in more detail.

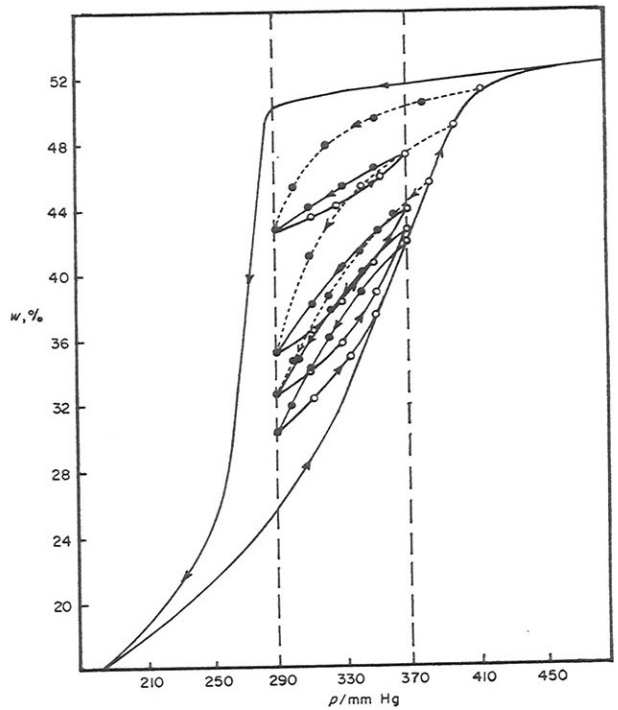

FIG. 36-16. Xenon on porous glass at 157.7°K. Subsidiary loops between the same limiting pressures at various positions in the main loop (*28*).

36-3. THEORIES OF ADSORPTION HYSTERESIS

A. Some General Thermodynamic Considerations

Before discussing the mechanism of adsorption hysteresis in detail it is important to lay down the basic thermodynamic requirements to which any theory of the phenomenon must conform. We consider, therefore, the thermodynamics of an experiment in which a very dilute gas (effectively at zero pressure) is confined in a cylinder that contains a sample of adsorbent; see Fig. 36-17. The piston is moved in reversibly under isothermal conditions,

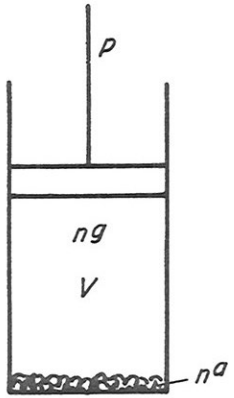

FIG. 36-17

until the saturated-vapor pressure is reached, and then out again, until the initial state is regained. We accept as an experimental fact that from a macroscopic point of view the adsorption isotherm is perfectly smooth and, consequently, during the uniform movement of the piston there is never an observable difference between the pressure exerted by the system and that applied to the piston. The work done by the surroundings on the system in any infinitesimal step in the cycle is

$$dW = -p\,dV \tag{36-1}$$

If the cylinder contains n^0 moles of gas, and if at a given pressure n^a moles are adsorbed, then (assuming for convenience that the vapor behaves as a perfect gas),

$$V = \frac{(n^0 - n^a)\mathbf{R}T}{p} \tag{36-2}$$

$$dV = -[(n^0 - n^a)\mathbf{R}T/p^2]\,dp - (\mathbf{R}T/p)\,dn^a \tag{36-3}$$

Thus we have

$$dW = (n^0 - n^a)\mathbf{R}T\,d\ln p + \mathbf{R}T\,dn^a \tag{36-4}$$

and in a complete cycle, from $p = 0$ to $p = p^0$ and back to $p = 0$,

$$\Delta W = \oint dW = -\mathbf{R}T \oint n^a\,d\ln p \tag{36-5}$$

Thus, if the curves of n^a versus $\ln p$ do not coincide along the adsorption and desorption paths—that is, if hysteresis occurs—the area of the loop, multiplied by $\mathbf{R}T$, will measure the decrease in the potential energy of the surroundings in one cycle. Assuming that all the components of the system and, in particular, the adsorbent return to their initial states, the cycle must have been accompanied by an irreversible entropy production (*29*) given by

$$\Delta_i S = \mathbf{R} \oint n^a\,d\ln p \tag{36-6}$$

This will have been manifested by an inequality between the heat given out by the system in the adsorption process (ΔQ_{ads}) and that taken in during the desorption process (ΔQ_{des}):

$$|\Delta Q_{\text{ads}}| - |\Delta Q_{\text{des}}| = T\,\Delta_i S \geqslant 0 \tag{36-7}$$

A fundamental requirement of any valid theory of adsorption hysteresis is, therefore, that it must provide an adequate description of the molecular processes that give rise to the entropy production.

B. The Domain Concept

Consideration of the thermodynamic requirement given above and the fact that the isotherms remain smooth on a macroscopic scale leads to the broad conclusion that the irreversibility must manifest itself in a series of microscopic irreversible processes, each of which is too small to be detected individually.† The simplest concept which can account for this behavior is that the system may be treated as an assembly of microsystems (domains), each of which can undergo irreversible transitions (*31*). The smoothness of the experimental curves then follows, if it is supposed that the characteristic values of x at which domains undergo these transitions differ from one domain to the next. This implies, as we shall see, that along the adsorption and desorption paths the system passes through different sets of microscopic molecular states.

Before discussing the detailed mechanism of domain processes it is useful to examine in general thermodynamic terms the origin of the irreversibility in individual domains. A spontaneous, thermodynamically irreversible change of state can occur in any microsystem which, when the chemical potential of

† In magnetic hysteresis the microscopic irreversible transitions can be detected by the Barkhausen effect (*30*).

the adsorbed component (measured by the vapor pressure it exerts) is plotted against the amount adsorbed, yields an S-shaped isotherm; see Fig. 36-18. When the chemical potential of the vapor is raised by an increase in its pressure, the system follows the curve *ABC*. At *C* a further increase in *p* leads to a situation in which only one state of the system is possible, namely *D*. The change from *C* to *D* occurs spontaneously. The adsorbed phase follows the path *CGD*, while the vapor maintains a constant chemical potential, because the amount of vapor taken up by a microscopic system

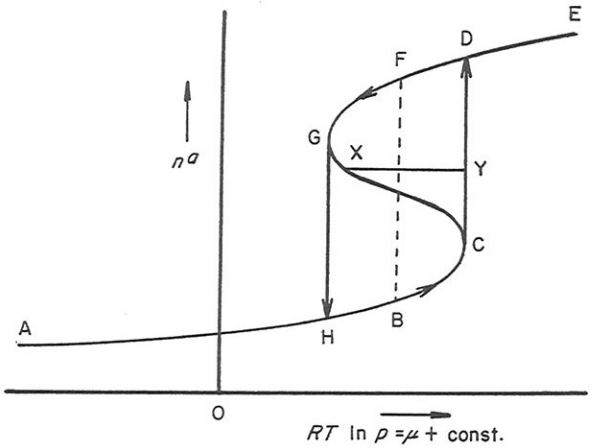

FIG. 36-18. Dependence of amount adsorbed (n^a) on $RT \ln p$ for a microsystem or a domain exhibiting metastability.

will be negligible compared with the total amount in the gas phase. At any instant the chemical potential of the vapor will exceed that of the adsorbed phase by *XY*: this difference is the affinity of the change (*32*), and the entropy produced in the irreversible change from *C* to *D* is given by

$$\Delta_i S = \frac{1}{T}\int_C^D (\mu^{\text{vap}} - \mu^{\text{ads}})\, dn^a \qquad (36\text{-}8)$$

The integral is simply the area of the loop *CGDC*.

Similarly, if the phase represented by the curve *EF* persists to *G*, then on a reduction in vapor pressure the desorption process will proceed along the route *EFGH*, in which the step *GH* will be irreversible and lead to an entropy production of $1/T$ (area *CGHC*); the total entropy production in a complete cycle will then be $1/T$ (area of the loop *HCDGH*).

In general, there will be points *B* and *F* on the isotherm, between which a reversible process involving the coexistence of two phases in equilibrium can

take place. In considering a detailed mechanism of the hysteresis it is necessary to explain why the system does not take this reversible route but passes through a series of one-phase metastable states. In certain cases the position of BF may be found from the classical "equal area" theorem; in other cases there may not be a single continuous curve between the two states of the system (*33*).

For simplicity we have supposed that beyond *B* the metastable state persists up to *C*; conversely, in desorption the metastable state beyond *F* does not break down until the point *G* is reached. It may well happen that for various reasons the metastable states break down before they become absolutely unstable. This does not affect the general argument but draws attention to the importance of nucleation processes in hysteresis phenomena.

C. Generalized Phase-Change Theories

As discussed in the preceding section, the fundamental requirement of a theory of adsorption hysteresis is that it shall indicate a mechanism whereby the system can undergo in limited regions a spontaneous, thermodynamically irreversible change of state. In principle, any process that gives rise to curves of the kind shown in Fig. 36-18 can exhibit the required behavior, provided that some mechanism exists which prevents the system from following an equilibrium path.

First we suppose that the material adsorbed in each elementary volume of adsorption space satisfies an equation of state of the van der Waals type. Because of the adsorption forces the density of the material will be greater near the surface than in the gas phase. Provided that the temperature is below a critical value, then, as the vapor pressure is increased, the density of material in any region of pore space will reach a value at which condensation to liquid should take place. If nucleation is needed to bring about this transition, the condensation process may be delayed (*34*). A metastable gaslike phase may persist and transform irreversibly to liquid. Similarly, on desorption the reverse process of evaporation may again be inhibited by the lack of a nucleation mechanism, and the system may pass through a series of metastable states (*31a*).

A discussion on these lines cannot, however, be developed without consideration of the surface-tension effects that come into play when liquidlike material is formed in the pore space. When these are considered we obtain the capillary condensation theory, which is discussed in detail in a later section.

Alternatively, the adsorbed phase may be pictured at low concentrations as a two-dimensional gas, which can be described by a two-dimensional equation of state of the van der Waals type. A surface phase change, analogous to those observed in films spread on a liquid surface, could be accompanied by metastability and hence lead to hysteresis.

Thirdly, multilayer formation may proceed through metastable states. According to Hill (*35*), when the BET theory is refined by taking account of lateral interaction and is applied to adsorption limited to a few layers, curves of the form shown in Fig. 36-19 are obtained. The transitions to monolayer coverage and then from one layer to two layers, etc., could, if conditions for nucleation were not favorable, proceed through metastable states and provide a mechanism of hysteresis.

The last two possibilities suggest that hysteresis might occur in the region of the isotherm in which the adsorbed material is in the process of taking on

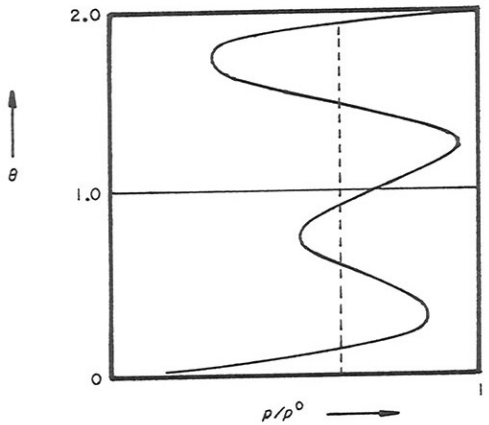

FIG. 36-19. Dependence of amount adsorbed (θ), in units of monolayer capacity, on relative pressure for adsorption limited to two layers (*35*).

liquidlike properties. If this kind of hysteresis occurred, it would probably be observed at lower vapor pressures than those associated with capillary condensation. It would not, however, be expected to persist to very low pressures and is unlikely to provide an explanation of the low-pressure hysteresis in systems showing type C or D behavior.

Furthermore, neither of these theories indicates the way in which the hysteresis is dependent on the pore structure of the solid. If phase changes of these kinds occurred on plane surfaces, one might expect hysteresis to be observed; the experimental evidence suggests that, when these phase changes take place on such adsorbents, they do so reversibly.

D. Capillary Condensation Theories

The older theories of adsorption hysteresis link the phenomenon with condensation and evaporation processes in the voids of a porous medium; they are classed as capillary condensation theories. The basis of the concept

of capillary condensation is the classical Kelvin equation (*36*), which relates the vapor pressure p over a curved meniscus to the mean radius of curvature r_m of the meniscus and to the surface tension σ:

$$\mathbf{R}T \ln p/p^0 = -2\sigma v \cos\theta/r_m \tag{36-9}$$

where p^0 is the saturated-vapor pressure of a bulk sample of the liquid, v is its molar volume, and θ is the contact angle of the meniscus at its line of contact with the solid, measured through the liquid phase. The mean radius of curvature is defined by

$$2/r_m = 1/r_1 + 1/r_2 \tag{36-10}$$

where r_1 and r_2 are the principal radii of curvature of the liquid–vapor interface.† There are two important limiting cases. For a spherical meniscus of radius r_{sph} we have $r_1 = r_2 = r_{\text{sph}}$, and so $r_m = r_{\text{sph}}$, and for a cylindrical meniscus of radius r_{cyl} we have $r_1 = r_{\text{cyl}}$ and $r_2 = \infty$, and so $r_m = 2r_{\text{cyl}}$. We shall not discuss the unresolved problem of the applicability of the Kelvin equation to the case in which the radii approach a few times the molecular diameter. It may be commented, however, that although there will, no doubt, be quantitative deviations from this equation (and these deviations may be quite large), the fundamental molecular kinetic factors that lead to this equation for macroscopic systems will still manifest themselves in microscopic systems.

The earliest theory of Zsigmondy (*7*) postulated that hysteresis was to be associated with different contact angles of a liquid in a cylindrical capillary during the condensation and evaporation processes. According to Zsigmondy's view, this difference is caused by the presence of impurities on the solid surface, which are displaced during adsorption. This implies that, once these impurities have been displaced, the solid surface will attain constant properties, and reversible adsorption should be observed. It is often found that the first one or two cycles of an adsorption hysteresis study yield results somewhat different from those of later cycles, and in some cases hysteresis can be eliminated in this way (*37*). Usually, however, the hysteresis loop settles down to a reproducible shape that persists for an indefinitely large number of cycles. In the work of Rao (*38*), for example, some of the experiments were continued for thirty cycles. Zsigmondy's theory may well explain the initial variability of the hysteresis loop, but the persistence and reproducibility of adsorption hysteresis loops, even after the most rigorous outgassing, is strong evidence against the view that the phenomenon is caused primarily by impurities. Contact-angle hysteresis is well known, however, in the movement of the line of contact of macroscopic liquid–solid–vapor interfaces, and there is evidence that this phenomenon,

† r_1 and r_2 are taken as positive if the corresponding centers of curvature lie in the vapor phase.

although influenced strongly by the presence of impurities, is not always eliminated in carefully purified systems. The necessary conditions for this type of hysteresis have still not been fully explored (*39*), so that one cannot yet entirely reject contact-angle hysteresis as a possible contribution to adsorption hysteresis. It should be noted, however, that contact-angle hysteresis is normally observed when a liquid–solid–vapor line of contact moves across a surface under the influence of hydrostatic forces, whereas the movement in a condensation process is controlled by a chemical potential gradient across the vapor–liquid interface; the two situations may not be strictly comparable, especially when the condensation process takes place in regions of microscopic dimensions.

Foster's (*40*) views on adsorption hysteresis were based on a consideration of the mechanism of meniscus formation in the adsorption process and of meniscus disappearance in desorption. These mechanisms were supposed to differ, and his theory is sometimes called the *delayed meniscus theory*. The ideas were applied to the simple case of an open-ended cylindrical capillary by Cohan (*10*); this development of Foster's theory, called the *open-pore theory*, is often regarded as the quantitative expression of his ideas. However, by considering only one simple pore geometry the more general aspects of Foster's work are concealed. In fact, the ideas expressed by Foster, although not developed in a detailed quantitative fashion by him, do in fact seem to contain most of the elements necessary for a satisfactory theory of capillary condensation hysteresis. We shall not, therefore, follow closely the expositions of Foster and Cohan but, rather, adopt a more general approach, which embraces their work and leads naturally to the so-called ink bottle theory of Kraemer (*41*) and of McBain (*42*).

Condensation in a closed tapering capillary should occur reversibly (*43*); see Fig. 36-20. As the partial pressure of vapor is increased, the adsorbed layer builds up, until it takes on liquidlike properties. At this point the sharply curved surface at the base of the capillary will ensure that, as the partial pressure of vapor increases, further adsorption will occur preferentially at the base. A meniscus is formed, which extends steadily up the capillary, until the pore space is full and the condensed liquid is bounded by a plane liquid surface exhibiting the saturated-vapor pressure of bulk liquid. It is possible that the vapor pressure at which the adsorbed layer takes on liquidlike properties (that is, develops a surface tension) may be higher than that corresponding to the minimal radius of curvature at the base of the capillary; if this is so, then the condensation that initiates the process of capillary condensation through the formation of a meniscus may be spontaneous. We shall not, however, consider this a significant contribution to the hysteresis phenomenon. Evaporation from a tapering capillary should proceed through the same series of meniscus configurations as did the condensation process.

By contrast, condensation in an open-ended cylinder always involves an irreversible step. When the adsorbed layer on the inside of a cylinder develops a surface tension, the cylindrical film, which exerts a vapor pressure corresponding to a meniscus of mean radius of curvature equal to the *diameter* of the cylinder [cf. (36-10)], becomes unstable with respect to an unduloid† containing the same amount of material (*44*). If the vapor pressure is maintained constant, then this unduloid is unstable with respect to unduloids containing more material. As the unduloid grows, Fig. 36-21a,b,c, its mean radius of curvature decreases, and spontaneous condensation continues,

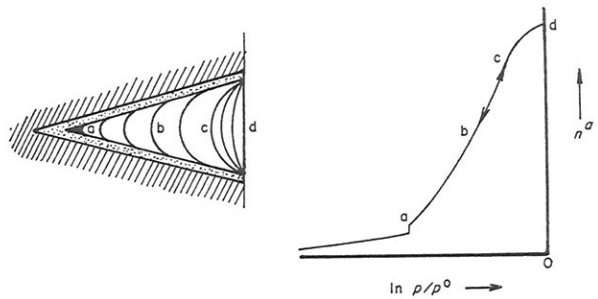

FIG. 36-20. Condensation in a closed tapering capillary. (a) Progress of meniscus in condensation and evaporation. (b) Variation of n^a with $\ln p/p^0$. Stippled area: adsorbed layer; blackened area: possible region in which some spontaneous condensation may occur.

until the pore is blocked by a biconcave lens of liquid, Fig. 36-21d. The condensed liquid, bounded by hemispherical menisci whose mean radius of curvature equals the *radius* of the cylinder, still has a lower chemical potential than the vapor, and spontaneous filling of the cylinder occurs, until the radii of curvature of the menisci at its ends are both equal to the *diameter* of the cylinder, Fig. 36-21e,f. If the vapor pressure is subsequently raised to p^0, the radius of curvature of the meniscus increases, until at p^0 it becomes infinite (plane surface), as shown in Fig. 36-22g. Evaporation from the body of the cylinder can now occur only when the vapor pressure is lowered to that corresponding to a meniscus of radius of curvature equal to the radius of the cylinder. Evaporation from the capillary will proceed reversibly until the point at which the two menisci meet "back to back" and the film between

† An unduloid is the surface generated when the curve traced by the focus of an ellipse rolling along a straight line is rotated about this line. The mean radius of curvature of an unduloid is the same at all points on its surface and is equal to the length of the major axis of the generating ellipse. The change in mean radius of curvature as condensation proceeds has been calculated and discussed by Haynes (*45*).

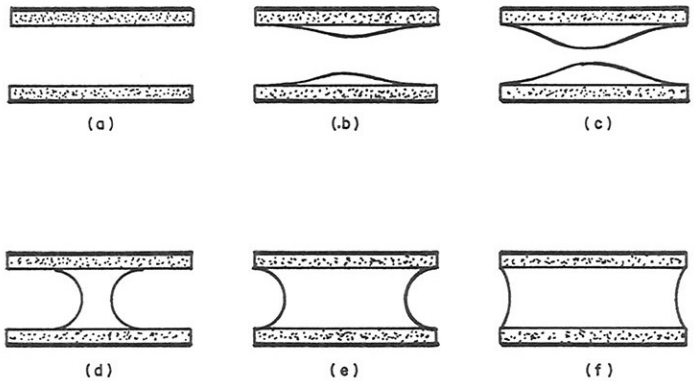

FIG. 36-21. Condensation in a cylindrical capillary; states (a) to (f) are described in text.

them bursts; see Fig. 36-22. Figure 36-23 shows the progress of the condensation and re-evaporation in terms of the chemical potentials of the vapor and condensed liquid; the condensation and evaporation paths differ from each other, and the open-ended capillary behaves as a domain in the sense employed above.

This simple example has been discussed in some detail because it illustrates the important principle that if the condensed phase reaches an unstable state relative to vapor held at constant pressure, then spontaneous condensation will occur, until the system finds a new state of equilibrium in which the mean radius of curvature of the surface corresponds to the ambient vapor pressure.

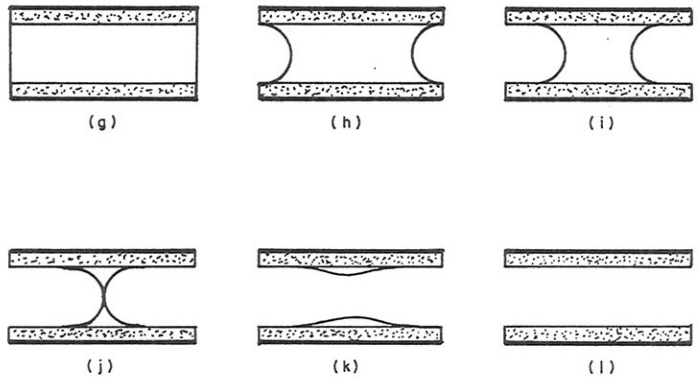

FIG. 36-22. Evaporation from a cylindrical capillary; states (g) to (l) described in text.

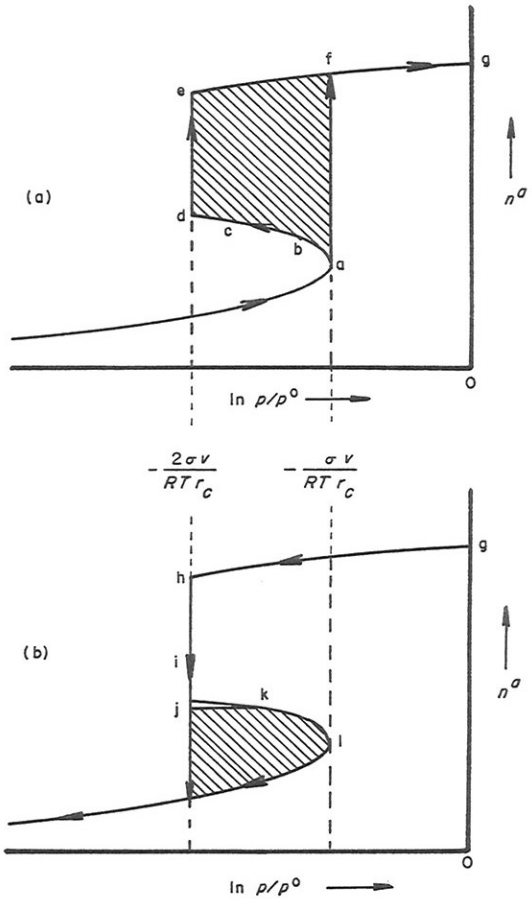

FIG. 36-23. Dependence of amount adsorbed on ln p/p^0: (a) for condensation in cylindrical capillary, (b) for evaporation from a cylindrical capillary. Letters denote states shown in Figs. 36-21 and 36-22. Shaded areas: contribution to entropy production.

It has been popular to discuss hysteresis in nonuniform capillaries in terms of the so-called *ink-bottle theory* attributed to Kraemer (*41*) and McBain (*42*). Here again it is common for this theory to be presented in specialized terms, which obscure the generality of the original ideas. Kraemer said: "It seems more likely that hysteresis is due to capillary spaces with narrower communicating channels. When the larger spaces are completely filled with liquid, desorption from them is retarded by the low vapor pressures over the

menisci in the narrow channels, just as a bottle with a capillary neck would fill at a high vapor pressure but would begin to empty only at a lower pressure." McBain's explanation† was that in a pore of nonuniform cross section "as the relative humidity of the vapor is gradually increased, condensation of

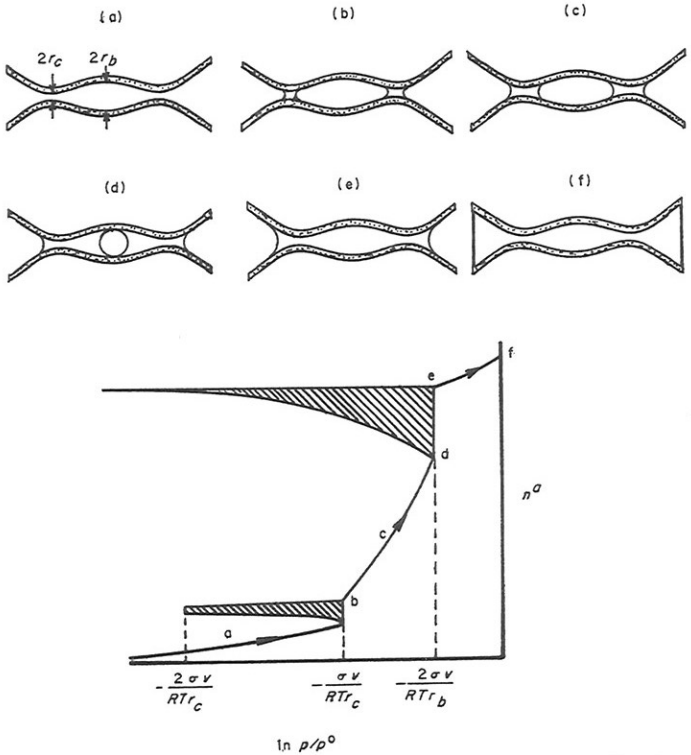

FIG. 36-24. Condensation in nonuniform capillary and (below) corresponding dependence of amount adsorbed on $\ln p/p^0$. Shaded area: contribution to entropy production.

liquid will begin at the narrowest cross section and will extend to wider cross-sections only as the relative humidity is increased, until when the vapor is sufficiently nearly saturated the pore will be completely filled. Upon subsequent diminution of the relative humidity . . . no evaporation will occur from this particular pore until the relative humidity has fallen to the value corresponding to the largest orifice or passage leading to the larger enclosed

† According to McBain these ideas were "suggested in discussion with a class on adsorption at Stanford University."

cavities." A macroscopic analogy involving the use of a narrow-necked bottle is then discussed, but both McBain and Kraemer use the bottle concept only as an example to illustrate the physical mechanism. They both clearly had in mind interconnected pore spaces rather than discrete bottles†. It seems that both authors envisaged an irreversibility associated with the desorption process, and in Brunauer's account of this theory (*46*) he says: "In this theory true equilibrium corresponds to the adsorption points since the important part of the liquid, that contained in the body of the pore, is in equilibrium with the vapor only on the adsorption side, but not on the desorption side." This statement is often repeated, but in fact it has a clear significance only when related to a specific pore geometry; it is not true, for example, in the case of the open-pore system discussed above. If we consider the condensation-evaporation cycle for a pore system such as that shown in Fig. 36-24, we see that condensation in the narrow sections will be delayed but, once it has commenced, it will proceed spontaneously, not only in the narrowest part, but also in wider regions in which the surface can adopt a configuration of mean radius of curvature less than the *diameter* of the neck in which condensation began. Irreversibility will be associated not only with this part of the condensation process but also with the final collapse of the vapor bubble formed when the two menisci developing from neighboring constrictions meet; see Fig. 36-24c,d. The latter contribution does not seem to have been previously discussed. The condensation and evaporation processes are shown separately in Figs. 36-24 and 36-25. The accompanying chemical potential diagrams indicate the paths followed in the condensation and evaporation processes; the shaded areas denote the contribution to the entropy production in these processes. Thus, in general, it is necessary in any realistic theory of capillary condensation hysteresis to combine the essential features of Foster's theory and of the ink-bottle theory. This point seems to have been first appreciated by Katz (*47*).

It must be stressed that irreversibility in the evaporation step depends on the inability of bubbles of vapor to form within the capillary condensed liquid.‡ If nucleation of bubbles occurred, then no irreversibility would be associated with the evaporation process.

The example shown in Figs. 36-24 and 36-25 shows immediately that the condensation-evaporation characteristics are controlled not only by the "pore-size distribution" but to a major extent by the topographical sequence of wide and narrow pore spaces. The so-called pore-size distribution curves obtained by the analysis of desorption isotherms involve, in fact, two statistical functions rather than one.

† Neither writer described the bottles as *ink* bottles, and it is not clear who first added the adjective; cf. Brunauer (*46*), p. 398.

‡ This is also mentioned by McBain (*42*).

The pore systems discussed above have been thought of as essentially one-dimensional arrays. Real systems will, of course, consist of three-dimensional networks. The particular case of the voids in a regular packing of spheres of equal size has been studied extensively. Although exact treatments are

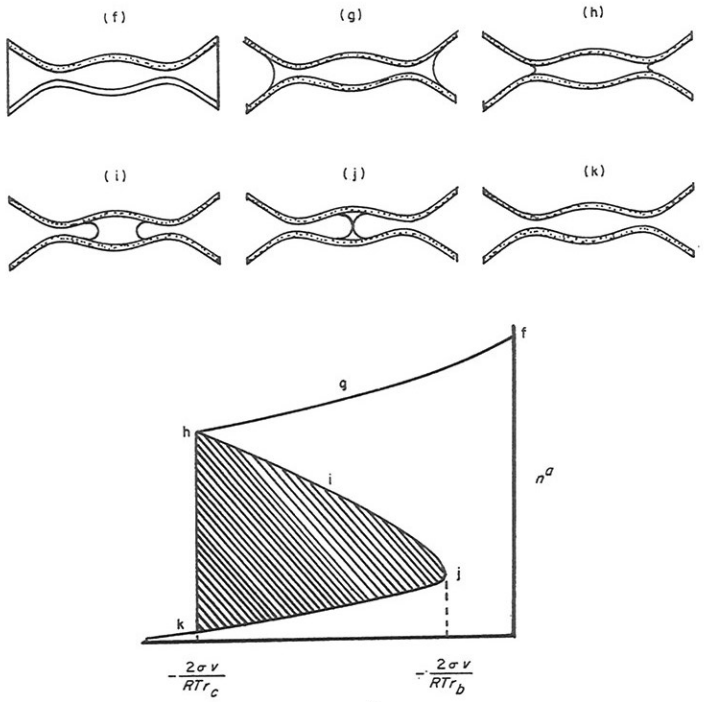

FIG. 36-25. Evaporation from a nonuniform capillary and (below) corresponding dependence of amount adsorbed on $\ln p/p^0$. Shaded area: contribution to entropy production.

mathematically intractable, several approximate calculations of the condensation-evaporation characteristics of packed spheres have been published (*48*). The case of random sphere packing is even more difficult to treat analytically.

A valid theory of adsorption hysteresis must account satisfactorily for the range over which the hysteresis loop persists and, in particular, for the dependence of the closure points on the properties of the adsorbate, the temperature, and the adsorbent structure. The capillary condensation

theory accounts readily for the upper closure point in terms of the pore structure of the solid, for if the upper closure point lies below the saturation pressure of the adsorbate vapor, then it may be presumed that the solid has no pores of radii greater than that corresponding to the closure point.† Adsorption beyond this pressure will be associated with the change of curvature of menisci freely accessible to the vapor.

It seems unlikely that similar considerations are applicable to the lower closure point. Only in very special cases is it likely that the lower closure point can be identified with adsorption in the smallest pores that exist in the material. A strong argument against this interpretation is that the relative pressure at which the loop closes is usually more characteristic of the adsorbate than of the adsorbent. It appears that, provided the solid has pores ranging down to and beyond some critical size determined by the properties of the adsorbate, then the same lower closure point will be observed for a range of adsorbents having different pore-size distributions.

The role played by the adsorbate in determining the lower closure point can be interpreted in at least two ways. According to the views of Foster and Cohan, condensation will not occur spontaneously until the adsorbed film has developed a surface tension. At this point the adsorbed phase ceases to behave as a single interphase between the vapor and the solid and takes on the character of a film having both an interfacial tension between the film and the solid and a surface tension characteristic of the liquid at the film–vapor interface. If, for example, it is postulated that the adsorbed film takes on liquidlike properties when a complete monolayer is adsorbed (this corresponds roughly to the assumptions of the BET theory), then one may deduce that hysteresis cannot occur in capillaries whose radii are less than about twice the diameter D of the adsorbed molecules.‡ The critical radius and, hence, the lowest vapor pressure at which hysteresis is possible will thus be controlled by the size of the adsorbate molecule. It is certainly observed that for many systems the amount adsorbed at the lower closure point is close to the "monolayer capacity" as derived from the BET equation or by the B-point method (cf. e.g., Fig. 36-5). Furthermore, calculations of the critical pore radius with the use of the Kelvin equation often lead to values not very different from twice the estimated dimensions of the adsorbate molecule. However, in finely porous systems the significance of the monolayer capacity

† In systems with a complex pore geometry the vapor–liquid surface may have principal radii of opposite sign, so that the mean radius of curvature is much larger than the dimensions of the actual pore spaces. If effects of this kind intervene, then even a finely porous material may not exhibit capillary condensation until a high relative vapor pressure is reached (*49*).

‡ Foster and Cohan give more detailed arguments leading to essentially the same conclusion (*10,40*).

is not very certain, while the quantitative use of the Kelvin equation in this range of relative pressures is highly suspect.

If it is assumed that the critical pore radius is independent of temperature, then, again using the Kelvin equation, the variation with temperature of $\ln p/p^0$ at the closure point can be calculated from the temperature coefficient of the quantity $\sigma v/T$. According to Dubinin and his co-workers (*26*), their data for the adsorption of CO_2 by silica gel are satisfactorily accounted for in this way. However, the rather slow variation of $\sigma v/T$ with temperature

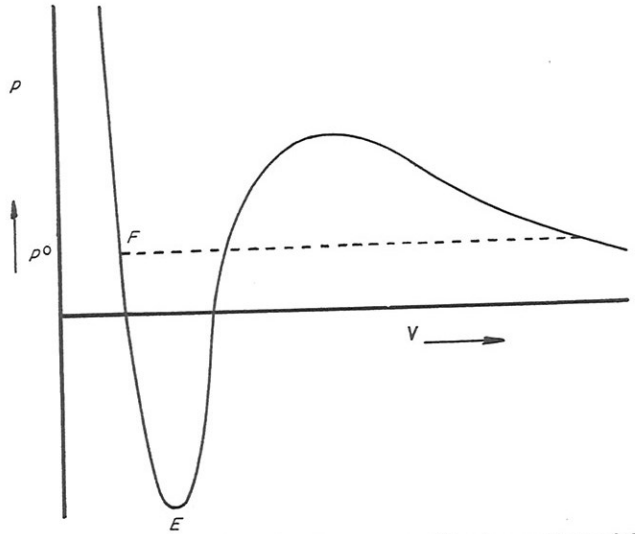

FIG. 36-26. Equation of state of liquid and vapor according to equations of the van der Waals type.

and the difficulty of establishing the exact closure point when the loops become small make this test difficult to apply with any precision.

An alternative consideration, to which rather little attention has been paid, is worthy of more detailed study (*50*). It has already been stressed that irreversibility in the evaporation step depends on the ability of the liquid to exist in a metastable state without the formation of bubbles in the capillary condensed liquid. Metastable states of this kind can occur in bulk liquid, provided that the liquid is free of dust particles or other nuclei, although there are few reliable experiments to establish the limits of this regime. Capillary condensed liquid is represented by states on the extension of the equation of state of the liquid into the metastable region corresponding to over expanded liquid, i.e., to states on the segment FE of Fig. 36-26. The range over which

these states can exist is always limited by the point E, beyond which the liquid state is thermodynamically unstable, but it may be further limited by the onset of bubble nucleation before the system reaches E.

We consider first the question of bubble nucleation. The critical bubble for evaporation of the liquid from the pores must have a vapor pressure just equal to that of the vapor and so must have a radius equal to that of the confining liquid interface. The possibility of forming a critical bubble may be controlled by geometrical factors, and the probability of forming a bubble

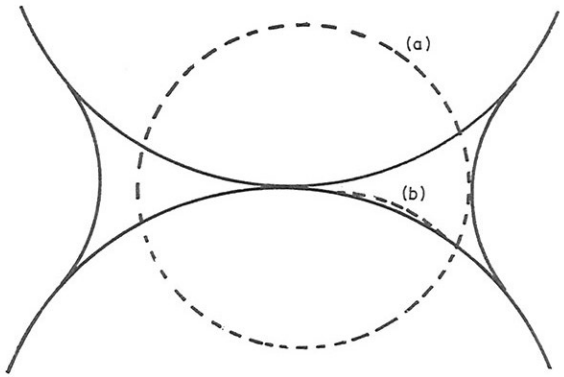

FIG. 36-27. Example of geometrical control of bubble nucleation. (a) Critical nucleus for bubble formation in bulk liquid. (b) Critical nucleus for bubble formation at solid surface.

will be controlled by kinetic factors. The probability of the spontaneous formation of a critical nucleus whose size is 10^{-6} cm or more is vanishingly small [cf. (*42*) and (*43*)] but increases rapidly for radii approaching 10^{-7} cm. Judging from the supersaturations required for the onset of spontaneous nucleation of water droplets from humid air, it seems likely that the critical bubble size at which the rate of nucleation becomes reasonable will lie in the range 10 to 20 A. Thus, the metastable liquid state in the pores may be expected to persist until p/p^0 has been reduced to a point corresponding to equilibrium with menisci of this radius. Experimental data certainly indicate limiting radii of about this size. On this view, the closure point of the hysteresis loop is not to be identified with the pore radius below which capillary condensation is impossible, but rather is it a measure of the critical nucleus size at which spontaneous bubble nucleation occurs. This distinction is important in the case of porous materials of varying pore section. Nucleus formation may also be controlled by geometrical factors. Thus, as an illustrative example, consider the situation shown diagrammatically in Fig. 36-27a.

At no stage in the retreat of the meniscus is it possible for a critical nucleus to appear: its radius is always larger than the space occupied by the condensed liquid. It may be suggested that a nucleus for evaporation might form on the capillary wall as shown in Fig. 36-27b. However, a nucleus of this shape implies that the liquid does not wet the surface of the wall. Although arguments based on macroscopic concepts may not be strictly applicable, it seems probable that a nucleus of the form shown will be physically incompatible with a concave liquid–vapor meniscus in the pore space.

If the breakdown of the metastable state is prevented by geometrical factors, then its existence will be limited only by the point E at which liquid under reduced pressure becomes unstable. At this point the adsorbed phase takes on a structure like that of compressed gas. The critical tension that the liquid can support will correspond to some critical pore size and so to a limiting relative pressure, below which capillary condensed liquid cannot exist. This lower limit will be a function of the nature of the liquid and of the temperature. Provided only that some pores of the limiting size are available in the adsorbent, the lower closure point will be independent of other details of the pore-size distribution.

The temperature dependence of the lower closure point will depend on the mechanism of the breakdown of the metastable state. If the nucleation mechanism operates, the limiting nucleus size will depend on kinetic factors, of which there is at present no adequate quantitative theory. On the other hand, if the metastable state persists over the whole range in which it is thermodynamically stable, then the limiting tension and, hence, the limiting relative pressure can be calculated, if the equation of state of the liquid is known. For the purposes of an illustrative discussion we may assume that the capillary condensed liquid follows a van der Waals equation of state. The dependence of the point E on temperature can then be calculated. It is readily shown that the limiting value of p/p^0 moves rapidly toward unity when the pressure corresponding to E changes over from negative to positive values. We shall expect the hysteresis loop to decrease in size rapidly in this temperature range. For a van der Waals liquid the pressure at E passes through zero when $T = 27T_c/32$ (*51*). For CO_2 these considerations would indicate a temperature of about 257°K, or −16°C, for the disappearance of hysteresis for this adsorbate; Dubinin and his co-workers report a value of about −20°C; see Fig. 36-10.

A detailed assessment of the ideas outlined above is not yet possible. There is a lack of suitable experimental data covering temperatures up toward the critical temperature. Furthermore, the critical pore sizes corresponding to the lower closure points, when calculated from the Kelvin equation, correspond to only a few molecular diameters, so there must always exist some doubt about the applicability of macroscopic thermodynamic arguments in this range.

Nevertheless, studies of the limits of hysteresis in capillary condensation may well provide an alternative method of studying the stability of liquids under tension.

E. Low-Temperature Hysteresis

So far the discussion has implied that adsorption is considered at temperatures at which the adsorbed phase can acquire liquidlike properties. However, hysteresis may also be observed at temperatures well below the triple point (*24,13*); see Fig. 36-9. For a short range below the triple point capillary condensation can persist because of the lowering of the triple point which is often observed in porous materials, but at lower temperatures a new hysteresis phenomenon appears and gives rise to a loop, whose size increases steadily with fall in temperature. Under these conditions the adsorbed phase will tend to take on solidlike properties. The precise structure of the solid will be determined by the interplay of the adsorption forces and those intermolecular forces between the adsorbed molecules which determine the structure of the bulk solid. When the amount of adsorption is small, the adsorption forces are likely to be dominant and will constrain the sorbate to adopt a structure compatible with the surface structure of the solid. When a sufficiently thick layer of adsorbed material has accumulated, however, new material may then adopt the crystal structure of the bulk solid adsorbate. Once this structure has begun to form, the phase boundary between this and the underlying structure may move back spontaneously toward the adsorbent surface. In desorption the reverse phase change may not occur at the same vapor pressure. The problems involved in a more detailed development of this theory are akin to those of epitaxy. Alternatively, the phase change can occur in two dimensions, as postulated in a special case by Amberg et al. (*24*); their theory may be regarded as a special case of the more general mechanism envisaged here. Hysteresis of this kind would be expected to exhibit an upper critical temperature, above which the two solid phases are indistinguishable, and to increase in extent as the temperature is lowered; both of these features have been observed.

F. Low-Pressure Hysteresis

None of the arguments presented so far can give a satisfactory account of low-pressure hysteresis. This phenomenon is usually attributed to irreversible intercalation of adsorbate within the structure of the solid. In many instances the solids involved (e.g., clay minerals and graphite) have a layer structure, and the postulate of interlamellar adsorption has been confirmed by observation (by X-ray methods) of the change of interlayer distance that accompanies adsorption (see e.g., *23,52*). Other materials that show similar hysteresis effects are more complicated in structure, but in most instances it

seems reasonable to postulate a penetration of the adsorbed species into the intimate molecular structure of the solid.

The following simple discussion of intercalation is capable of accounting qualitatively for most of the observed features of the phenomenon.

Consider the situation in which interlamellar penetration has commenced see Fig. 36-28. The driving force for this penetration is the spreading pressure

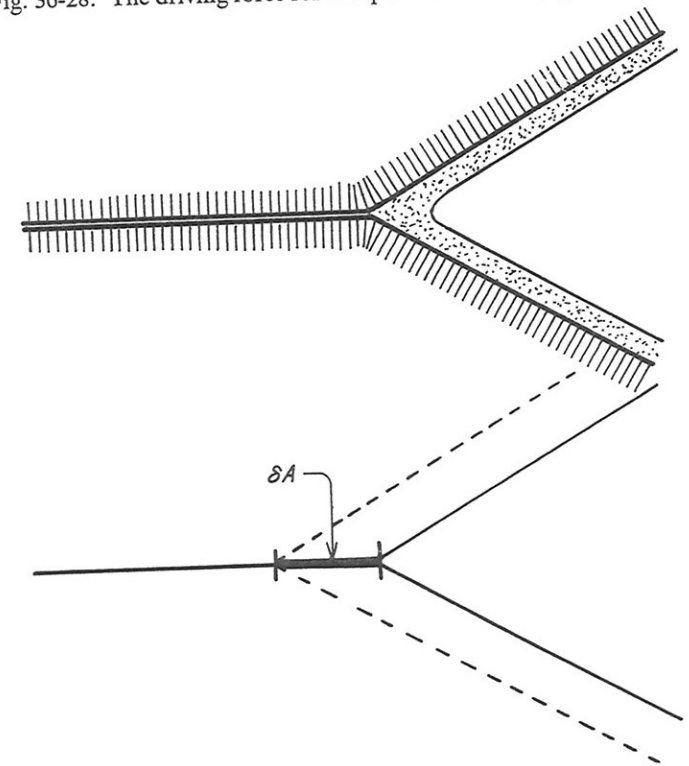

FIG. 36-28. Intercalation of adsorbed phase between layers of adsorbent.

of the adsorbed film, defined by

$$\phi = (\partial G/\partial A)_{T,p,n^a} \tag{36-11}$$

where G is the Gibbs free energy of the system. This is opposed by the cohesive forces of the solid structure. An increase in the depth of penetration will occur spontaneously, if the increase in free energy, which is needed to separate an additional area of the two solid surfaces against cohesive forces, is more than balanced by the decrease in free energy ($\phi\, dA$) resulting from the extension of the adsorbed phase. Penetration will occur if ϕ exceeds

some critical value. Because of powerful adsorption forces within the structure desorption of intercalated molecules may then occur only at a very low relative pressure. The quantitative development of this picture requires knowledge of the dependence of the free energy of the solid on the interlamellar spacing. This will depend on the detailed structure of the solid, and in many instances a dominant role may be played by the nature and distribution of defects in the solid structure. It is not unlikely that the first irreversible step is the "prising open" of the layers to admit the first few molecules of the adsorbate. The expanded solid may then adopt a new position of minimum structural potential energy, so that when the adsorbate is subsequently removed, the solid may not return to its initial state except after a long period at the experimental temperature or a shorter period of annealing at a higher temperature.

Since the spreading pressure is related to the adsorption isotherm through the equation

$$\phi = \mathbf{R}T\int_0^p n^a\, d\ln p \tag{36-12}$$

where n^a is the surface concentration of adsorbed matter, the postulate that there is a critical value of ϕ, which must be achieved before intercalation can occur, implies that there will be a threshold pressure for this phenomenon. Furthermore, this pressure will be temperature-dependent, so that in certain circumstances we may expect to find a temperature threshold below which ϕ never becomes large enough to cause penetration of the solid. We may also expect that whether or not low-pressure hysteresis occurs will depend on the cohesive strength of the solid structure: in weakly bonded solids penetration may occur reversibly, in very rigid structures it may not occur at all, and in intermediate cases irreversible relaxation of the solid may take place. This sequence has been observed in the adsorption of benzene by a series of porous carbons pepared from polyvinylidene chloride under a range of conditions leading to materials of varying structure (varying degrees of cross-linking) (*19*). Finally, low-pressure hysteresis will be strongly dependent on the molecular size of the adsorbate in relation to the interlamellar spacing. Very small molecules will intercalate easily, but in the case of much larger molecules the energy required to separate the layers enough for insertion of a molecule will be much greater than that which can be recovered from adsorption forces. Thus, certain coal carbons adsorb benzene reversibly in the temperature range 25 to 45°C. Adsorption of 2:2-dimethylbutane at 25°C is also free from hysteresis. At 45°, however, substantial low-pressure hysteresis is observed (*25*). In a similar way (cf. Fig. 36-7b) adsorption of benzene by certain polyvinylidene chloride carbons exhibits only "capillary condensation" hysteresis, whereas adsorption of *n*-hexane and cyclohexane by the same carbon is accompanied by low-pressure hysteresis (*19*).

An apparent exception to this prediction is found in the work of Saunders

et al. (*52*) on the adsorption of bromine from carbon tetrachloride solution by graphite. In this work it was found that the threshold concentration of bromine in solution increased with increase in temperature. In this case, however, it seems likely that the bonding of bromine to the graphite may be chemical in nature, and the picture developed here for physical adsorption may not be equally applicable to chemisorption processes from solution.

36-4. EXPERIMENTAL EVIDENCE FOR CAPILLARY CONDENSATION

Passing reference has been made to a number of experimental observations which are relevant to the theoretical interpretation of hysteresis phenomena,

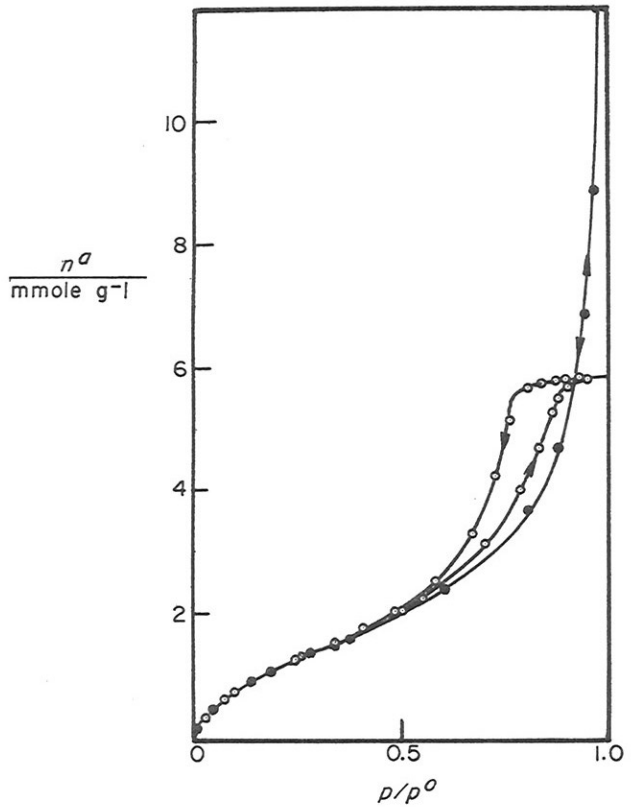

FIG. 36-29. Adsorption of CF_2Cl_2 at 33.1°C by Linde silica (●) as a loose powder and (○) as a compressed pellet. [Redrawn from (*55*) by permission of the Royal Society of London.]

and these will be considered in more detail later. It is convenient at this point, however, to consider separately those observations that provide direct evidence of the role played by the pore structure of the solid, and hence, we presume, by capillary condensation in hysteresis phenomena.

First, an experimental observation of long standing (*7,53*) is that when silica gel adsorbs a condensible vapor, the solid appears cloudy only over that range of relative pressures associated with the hysteresis loop. This light-scattering effect is evidence of the existence of density fluctuations in the adsorption space; it is probably to be attributed to the scattering of light by the large number of menisci present in the material during the capillary condensation phase, both on adsorption and in desorption. Unfortunately, no quantitative study of light-scattering by adsorbed phases has been carried out, although Coelingh (*54*) has used optical effects to examine hysteresis in water adsorption by a weathered-glass surface.

An important contribution to the establishment of the origin of capillary condensation was made by Carman and Raal (*55*), who showed that, whereas adsorption on an uncompressed nonporous powder exhibits reversible multilayer adsorption, the same powder in the form of a compressed pellet adsorbs only a limited amount of vapor, determined by the pore volume of the pellet, and shows hysteresis of the kind that we have identified as of the capillary condensation type; see Fig. 36-29. Recently experiments that are essentially the converse of those of Carman and Raal have been carried out by Bailey (*19*) who has shown that hysteresis loops of type B exhibited by porous carbons and by coconut shell charcoals are eliminated if the carbon is finely ground in an agate ball mill to pass 300 mesh. The adsorption isotherm is now reversible and falls somewhat above that shown by the solid samples; see Fig. 36-30. These experiments provide strong evidence that the structure of the carbon consists of highly porous adsorptive units exhibiting reversible adsorptive characteristics, packed together in a random manner. The larger voids between these adsorptive units are responsible for the capillary condensation hysteresis, which is eliminated when the void structure is destroyed by grinding. Electron micrograph studies have identified the adsorptive units as shrunken pseudomorphs of the original platelike crystals of the polymer from which the carbon was prepared (*19*). Further circumstantial evidence connecting adsorption hysteresis of types A and B with capillary condensation comes from the close similarity between the general characteristics of the adsorption phenomenon and the moisture wetting and draining of packed particulate beds (*56*). Data for the adsorption hysteresis of CF_2Cl_2 in a Linde silica plug (see Fig. 36-29) are compared in Fig. 36-31 with the water characteristics of plaster of Paris and packed sand. In this figure the tension in the water rather than vapor pressure is plotted logarithmically as the abscissa.

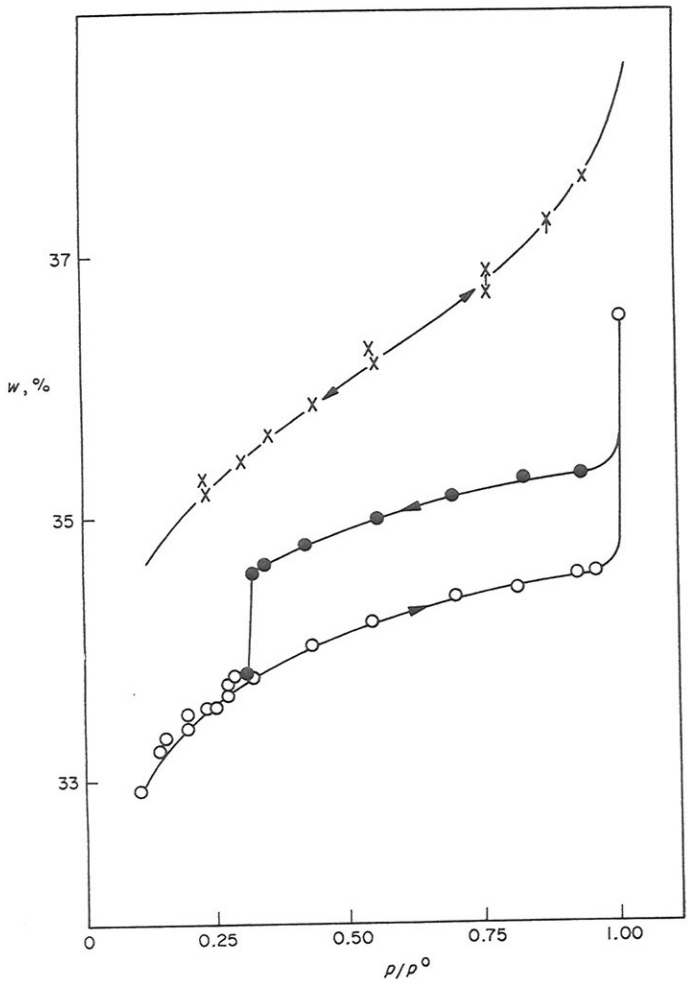

FIG. 36-30. Adsorption of benzene by polyvinylidene chloride char (○) as pellet and (x) after grinding to pass 300 B.S.S. sieve size (*19*).

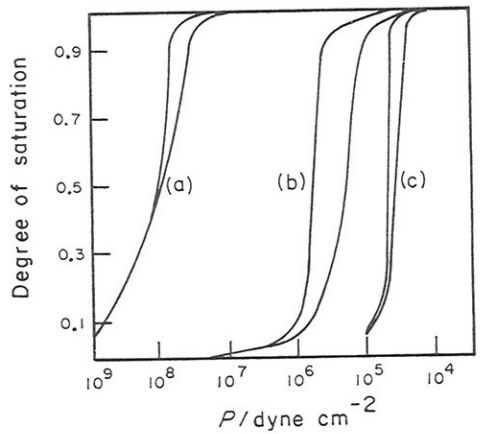

FIG. 36-31. Comparison of adsorption hysteresis in system CF_2Cl_2 plus silica plug (a), with wetting hysteresis of plaster of Paris by water (b), and sand-bed by water (c). P is the tension in the liquid phase. [Redrawn from (*56*) by permission of American Chemical Society.]

36-5. DOMAIN EFFECTS IN ADSORPTION HYSTERESIS

A. General Considerations

In the preceding section we examined some physicochemical mechanisms that can lead to the persistence of thermodynamically metastable states in individual "domains" in the adsorption space. The observed phenomena result, however, from the superposition of all such effects occurring in all parts of the system. We proceed now to discuss the way in which the total observable effects can be related to the individual domain processes and to outline a method of accounting for the complex behavior observed in scanning experiments.†

The domain theory can be developed in very general terms (*31*). For the present purpose, however, it is more useful to reformulate it so that it applies specifically to systems showing capillary condensation hysteresis, since the most extensive studies of hysteresis behavior have been made on systems in which this appears to be the most likely mechanism. The simplest form of the theory, in which the domains are presumed to behave independently of one another, is found to be inadequate to account for all the experimental observations, and we are led to develop an extended theory.

We first divide the whole adsorption space into individual "pore domains."

† The first attempt to discuss this problem and to deduce general rules governing scanning behavior appears to have been the work of Katz (*47*).

A convenient definition of a pore domain is a region of pore space accessible from neighboring regions through pore constrictions. In the simple case of the pore space formed by equal spheres in perfect close packing the pore domains may be identified with the so-called tetrahedral and octahedral holes, which are joined through "windows" consisting of triangular foramina. An isolated pore domain will, in accordance with the principles outlined above have well-defined condensation-evaporation characteristics involving one or more spontaneous irreversible steps. To describe the behavior of a pore domain in more detail we divide it into elements of volume, dV. At a given

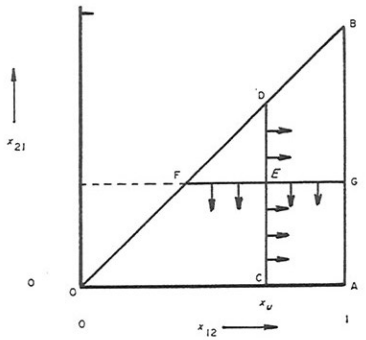

FIG. 36-32. Definition of domain properties in terms of x_{12} and x_{21}. See text.

stage in an adsorption-desorption cycle each element of volume will contain either liquid or vapor (the elements are supposed to be so small that we can ignore those which lie in the liquid–vapor interface). A given element of volume in an isolated domain then has the property that during an adsorption process a liquid–vapor interface will sweep through it at a certain relative pressure x_{12} and during desorption the interface will pass back through it, leaving it empty, at x_{21}. If the pore domain as a whole behaves irreversibly in the cycle, then $x_{12} \geqslant x_{21}$. The equality holds for elements in those regions which fill and empty in reversible sections of the process. We now classify all elements of volume in terms of the two characteristic quantities x_{12} and x_{21}, which we take as co-ordinates in Fig. 36-32. Because of the inequality given above, the points representing all elements of volume will lie in the triangle OAB. We now associate with each element of area $dx_{12}\,dx_{21}$ of this diagram a quantity $v(x_{12}, x_{21})$, such that $v(x_{12}, x_{21})\,dx_{12}\,dx_{21}$ is the volume of the pore domain associated with values of x_{12} and x_{21} in the ranges x_{12} to $x_{12} + dx_{12}$ and x_{21} to $x_{21} + dx_{21}$. The distribution function $v(x_{12}, x_{21})$ characterizes the properties of the pore domain.

B. The Independent-Domain Theory

In the *independent-domain theory* we assume that each pore domain behaves as though it were interacting with the vapor as an isolated pore; we can then sum the values of $v(x_{12}, x_{21})$ for all the pore domains comprising the system and characterize the whole system in terms of a *total* $v(x_{12}, x_{21})$ function, which defines the distribution of the filling-emptying properties of the whole system.† The adsorption-desorption properties of the system can now be described simply in the following way.

When a particular value of x (corresponding to C, Fig. 36-32) is reached during an adsorption process starting from zero pressure, all elements of volume for which $x > x_{12}$ will contain liquid, the total volume of which is given by

$$V = \int_0^x \int_0^x v(x_{12}, x_{21})\,dx_{12}\,dx_{21} \tag{36-13}$$

The function v is the total function mentioned above, which, according to (36-13) is integrated over the triangle OCD. If the values of $v(x_{12}, x_{21})$ are plotted vertically over the $x_{12}x_{21}$ plane, forming a surface over this plane, then V is the volume of the solid figure lying between this surface and the base plane over the triangle OCD. An adsorption process may thus be represented by the movement of a vertical line across the triangle from left to right, and at any point the state of the system may be represented by a diagram such as that in the lower row of Fig. 36-33a. Everett and Smith (*31b*) suggested the name *domain complexion* for diagrams of this kind.

At saturation, when $x = 1$,

$$V^s = \int_0^1 \int_0^1 v(x_{12}, x_{21})\,dx_{12}\,dx_{21} \tag{36-14}$$

where the integration is taken over the triangle OAB.

When a particular value of x (corresponding to G) is reached during a desorption process, starting from completely filled pores at $x = 1$, all elements of volume for which $x < x_{21}$ will have emptied. The volume of liquid remaining adsorbed will then be given by

$$V = V^s - \int_x^1 \int_x^1 v(x_{12}, x_{21})\,dx_{12}\,dx_{21} \tag{36-15}$$

The integral of $v(x_{12}, x_{21})$ over the triangle FGB is subtracted from that over the triangle OAB. The desorption process can thus be described in terms of the movement of a horizontal line from top to bottom of the triangle.

† Although we use the same symbol $v(x_{12}, x_{21})$ for the distribution function for a single pore domain and for the whole system, no confusion should arise, because in all that follows we shall be discussing the properties of the whole system.

During this process the state of the system is represented by diagrams such as Fig. 36-33b. If the adsorption process had been stopped at x_u, then the subsequent desorption would have followed a primary desorption scanning curve, the state of the system at any point being represented by diagrams such as Fig. 36-33c.

A primary ascending curve from a lower limit x_l will again be described by the movement of a vertical line starting from F (Fig. 36-32). At the start of this process all elements of volume whose representative points lie in $OAGF$

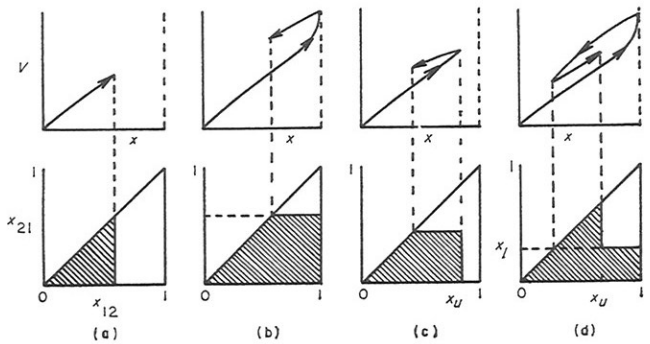

FIG. 36-33. (a) Adsorption boundary curve and corresponding domain complexion. (b) Desorption boundary curve and corresponding domain complexion. (c) Primary desorption scanning curve and corresponding domain complexion. (d) Primary adsorption scanning curve and corresponding domain complexion.

will already be filled; the ascending process will thus lead to the refilling of the volumes corresponding to the points in FED which were emptied in the preceding desorption. The state of the system may be represented by Fig. 36-33d.

Considerations based on the simple rules outlined above lead to the prediction of paths such as those shown in Figs. 36-34 and 36-35; these are the types of behavior found experimentally and illustrated in Figs. 36-13 and 36-14. Figure 36-35 shows that, if a given point in a loop is reached in two different ways, the domain complexions corresponding to the point have different shapes but are such that the integrals over the shaded areas have the same value. We see also why the path traced by the system, when it moves away from P, depends on the history of the system before it reached P. The domain complexion diagram thus performs the function of a memory in systems showing hysteresis.

This theory also emphasises that the slope of a curve immediately after a reversal refers to reversible changes in the system, for the elementary volumes

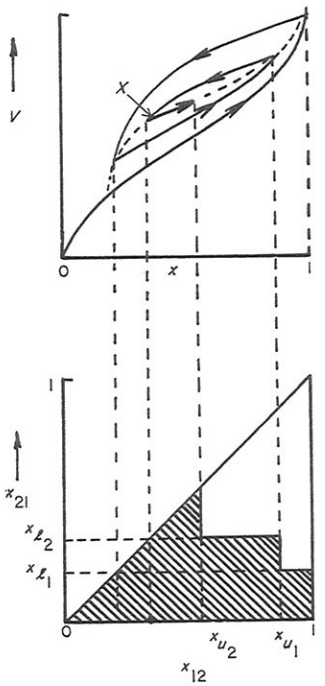

FIG. 36-34. Spiral path within hysteresis loop and corresponding domain complexions.

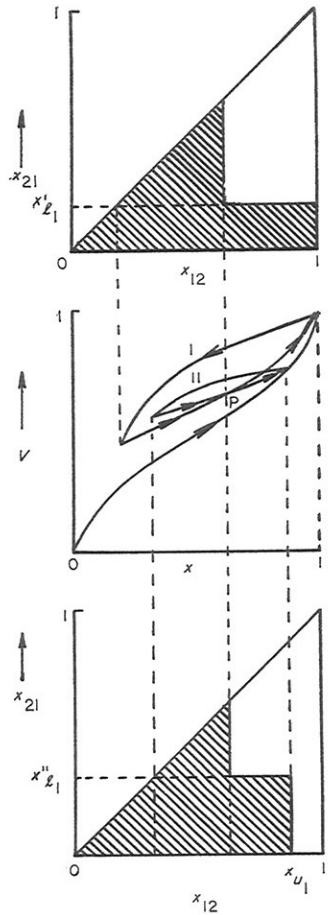

FIG. 36-35. Two routes, denoted by prime and double prime, to point P in hysteresis loop and corresponding domain complexions.

involved are those in a small triangle close to the line OB along which $x_{12} = x_{21}$, that is, along which the elements behave reversibly. Hence, if we approach (Fig. 36-36) a point Q (i) from above and (ii) from below and reverse both paths at Q, then the ascending curve from Q arising from (i) and the descending curve arising from (ii) should have the same slope. This has been confirmed experimentally by Blakeney-Edwards (*28*).

In general, it is found that all predictions of the theory related to considerations of the areas of the $x_{12}x_{21}$ plane, over which integration is performed, are verified experimentally. On the other hand, those predictions which involve the actual values of these integrals are of less general validity.

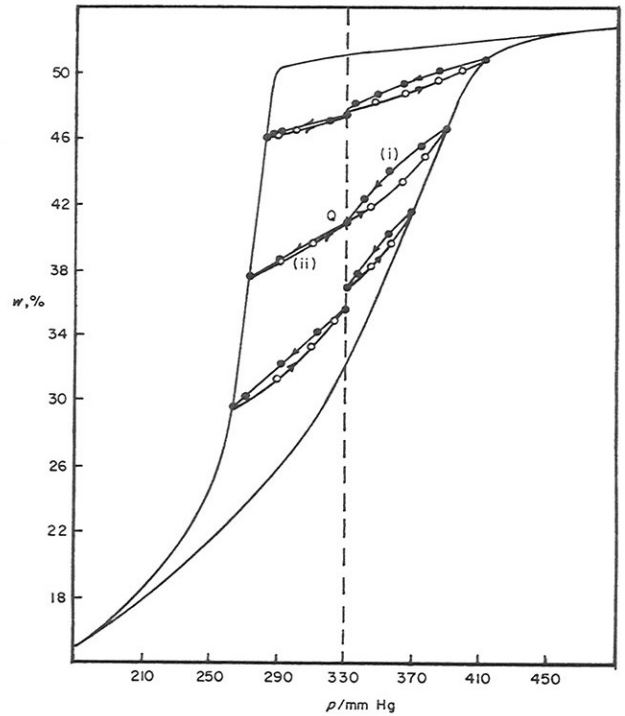

FIG. 36-36. Slopes of adsorption and desorption curves immediately after reversal at a given point (*28*). See text.

Before proceeding further we note that the properties of a system can always be expressed as the sum of integrals over triangles, all of whose hypotenuses are on the line OB. We adopt the following notation.

$$V(x_l, x_u) = \int_{x_l}^{x_u}\int_{x_l}^{x_u} v(x_{12}, x_{21})\, dx_{12}\, dx_{21} \tag{36-16}$$

That is, $V(x_l, x_u)$ is the integral of $v(x_{12}, x_{21})$ over the triangle whose hypotenuse lies on OB between x_l and x_u; see Fig. 36-37. We also adopt the convention that

$$V(x_l, x_u) = -V(x_u, x_l) \tag{36-17}$$

and a notation (*31d*) which summarizes, for a given point such as X in Fig 36-34, the history of the system. Thus, at X we write V as

$$V\begin{pmatrix} 1 & x_{u_1} \\ 0 & x_{l_1} \quad x_{l_2} \end{pmatrix}$$

where the values of x corresponding to upper bounds are placed above the line opposite V, and those corresponding to lower bounds, below the line.

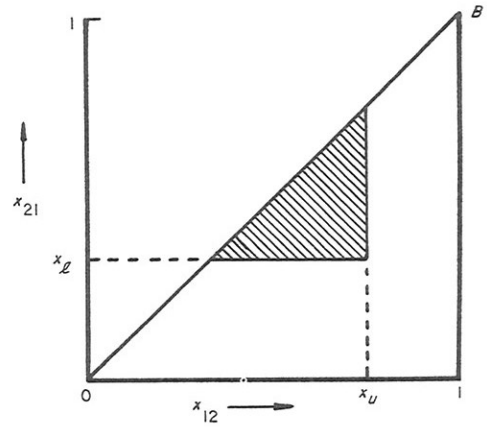

FIG. 36-37. Definition of function $V(x_l,x_u)$.

Then, for example, the volume of adsorbed liquid at X is

$$V\begin{pmatrix} 1 & x_{u_1} \\ 0 & x_{l_1} \quad x_{l_2} \end{pmatrix} = V(0,1) + V(1, x_{l_1}) + V(x_{l_1}, x_{u_1}) + V(x_{u_1}, x_{l_2}) \tag{36-18}$$

The slope of the descending scanning curve through X will be

$$\frac{dV}{dx} = \frac{dV(x_{u_1}, x)}{dx} \tag{36-19}$$

and will arise from the contribution to V from the horizontal black strip in Fig. 36-38. If we now compare the slopes of a series of descending scanning curves, of which two examples are shown in Fig. 36-38, then at any given value of x the slopes of curves starting from increasing values of x_u should also increase. In the same way the slopes at given x of a series of ascending scanning curves corresponding to decreasing values of x_l should increase; see Fig. 36-39.

It is usually found experimentally that the ascending scanning curves satisfy the requirements of the theory, but in many instances (*57,58*) the

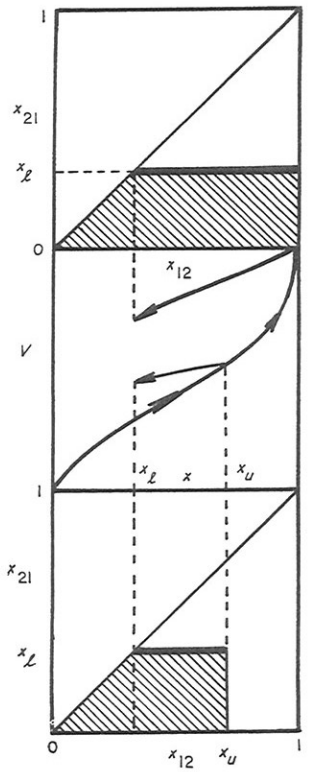

FIG. 36-38. Derivation of slopes of descending scanning curves.

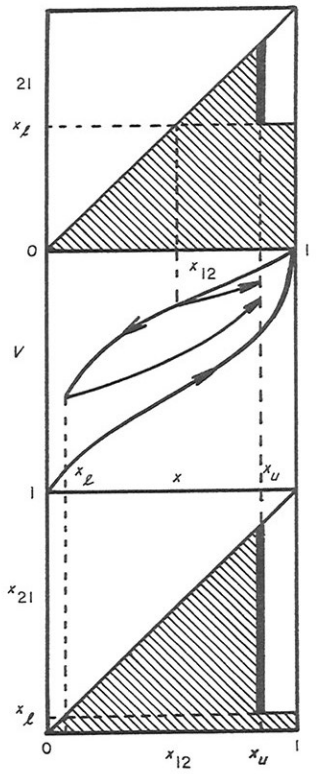

FIG. 36-39. Derivation of slopes of ascending scanning curves.

slopes of the desorption scanning curves at a given relative pressure *decrease* toward the top of the loop; see Figs. 36-12 and 36-16.

If we now consider a loop formed between the same values of x_l and x_u, then the ascending and descending segments will correspond, respectively, to the sweeping of the triangle FED (Fig. 36-32) by a vertical and a horizontal line. These processes should be independent of the form of the rest of the domain complexion diagram and, consequently, the loop shape should be independent of the position of the subsidiary loop within the main loop.† Everett and Smith's measurements of the adsorption of N_2O on coconut

† Enderby (*31d*) has used rather more general arguments to show that the loops need not be congruent: it is sufficient that the height of the loop at a given value of x should be independent of the position of the loop.

shell charcoal show closed internal loops of constant shape, but Quinn and McIntosh (*58*) found that for butane adsorbed on porous glass the internal loops high in the boundary loop were narrower than those lower down. Blakeney-Edwards (*28*) and Brown (*13*) have obtained similar results for xenon adsorbed on porous glass; see Fig. 36-16.

Finally, it should be possible (*31b,c*) to calculate the distribution of domain properties from a complete knowledge of *either* the primary adsorption scanning curves *or* the primary desorption ones. The theory can then be tested either by comparing the distribution functions derived from the two sets of measurements or by calculating one set of primary scanning curves from a knowledge of the other set and then comparing the calculated curves with those observed experimentally. Everett and Smith (*31b*) showed that for the system CO_2 plus charcoal the calculated curves agreed reasonably well with the experimental points, and the independent-domain theory has also been applied successfully to hysteresis in the wetting and draining of packed beds of sand and of glass spheres (*59*); the latter phenomenon is, of course, controlled by essentially the same mechanism as capillary condensation. However, the breakdown of the independent-domain theory in the adsorption on porous glass, noted previously, is confirmed by the more rigorous quantitative test (*28*).

The failure of the independent domain theory to account quantitatively for the behavior of many systems, especially those in which we expect the phenomenon to be controlled by capillary condensation processes, leads us to re-examine the assumption that the behavior of a domain is independent of the state of its neighbors.

C. Interdependence of Domain Processes

As stressed in Section 36-3D the condensation-evaporation behavior of a pore system of variable cross section is determined, not only by the statistical distribution of pore radii, but also by the sequence of constrictions and bulges. Thus, whereas in an isolated pore a given element of volume will fill and empty at given values of x_{12} and x_{21}, when the pore is interconnected with others this same element may or may not undergo these changes at the same values of x, depending on the way in which the pore is interconnected and upon whether the adjacent pores are full or empty (*pore blocking effects*). In general, therefore, the behavior of an element of volume will depend on the state of neighboring pores and, hence, on the history of the system as a whole. The influence of domain interactions on scanning behavior has been discussed by Enderby (*31d*) for the case of a linear array of domains. His analysis does not, however, lead to any very simple method of interpreting experimental data. In the following we develop a description which derives from the preliminary discussions of Everett and of Barker (*60*). A fuller account is in preparation.

To specify the properties of the system more completely, we introduce two functions p_{12} and p_{21}. Consider all elements of volume characterized by given values of x_{12} and x_{21}. The function p_{12} gives the fraction of those which have filled when under given conditions x has risen to a specified value, and p_{21} is the ratio of those which have actually emptied when x has fallen to a specified value under the given conditions to those which would have emptied if the pores had behaved independently. For the case of independent

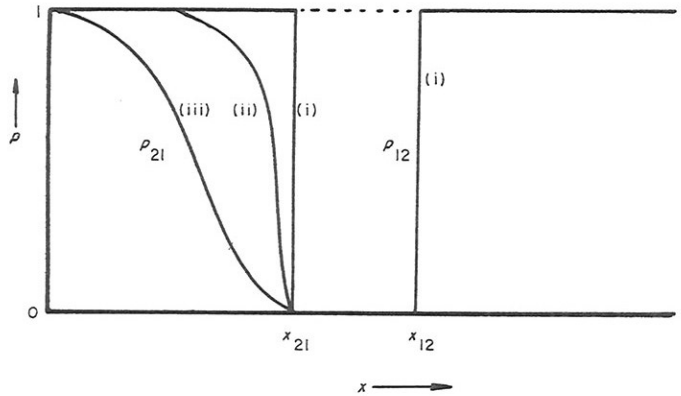

FIG. 36-40. Definition of the functions p_{12} and p_{21}. See text.

domains we have simply

$$p_{12} = 0, \quad x < x_{12}$$
$$p_{12} = 1, \quad x > x_{12} \qquad (36\text{-}20a)$$

$$p_{21} = 0, \quad x > x_{21}$$
$$p_{21} = 1, \quad x < x_{21} \qquad (36\text{-}20b)$$

These functions are shown as curves (i) in Fig. 36-40. In general, however, the functions p_{12} and p_{21} for a given group of domains will depend on x in a manner that depends on the state of filling of the neighboring domains. Consideration of the mechanisms discussed in Section 36-3D, supported by the experimental evidence that the slopes of the adsorption scanning curves do not contradict the predictions of the theory, leads us to expect that in most cases the empty-to-full transition will be relatively uninfluenced by pore interconnection, whereas the full-to-empty transition will be critically dependent on pore-blocking effects. For the present, therefore, in the first extension of the theory we shall assume that p_{12} satisfies equation (36-20a) and that p_{21} has the form shown in Fig. 36-40, curves (ii) or (iii). The form of p_{21} will deviate progressively from curve (i) as the degree of pore-blocking increases.

To keep the theory in a tractable form we assume that the pore-blocking effect is dependent on the total volume of the adsorbed liquid and that we need not attempt to specify in detail its precise distribution. We may thus write $p_{21}(x_{12}, x_{21}, x, V)$.

For the ascending boundary curve we have, as before,

$$V(0, x) = \int_0^x \int_0^x v(x_{12}, x_{21})\, dx_{12}\, dx_{21} \qquad (36\text{-}21)$$

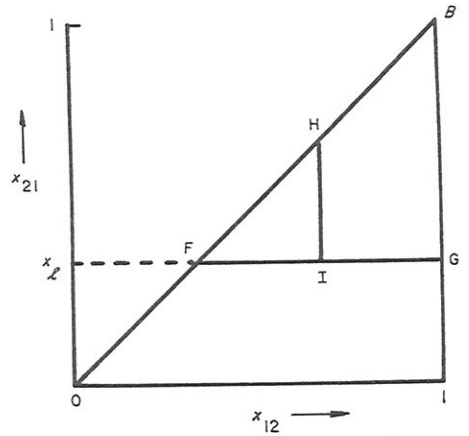

FIG. 36-41. See text for explanation.

Along the descending boundary curve the contribution of a given element of the domain complexion diagram to the decrease in the amount adsorbed will be†

$$dV = p(x_{12}, x_{21}, x, V)\, v(x_{12}, x_{21})\, dx_{12}\, dx_{21} \qquad (36\text{-}22)$$

so that the descending curve is given by

$$V\begin{pmatrix} 1 & \\ 0 & x \end{pmatrix} = V(0, 1) + \int_1^x \int_1^x p(x_{12}, x_{21}, x, V)\, v(x_{12}, x_{21})\, dx_{12}\, dx_{21} \qquad (36\text{-}23)$$

We now consider the average value of p for all elements of the system represented by points in the triangle FGB (Fig. 36-41):

$$P = \frac{\int_1^x \int_1^x p(x_{12}, x_{21}, x, V)\, v(x_{12}, x_{21})\, dx_{12}\, dx_{21}}{\int_1^x \int_1^x v(x_{12}, x_{21})\, dx_{12}\, dx_{21}} \qquad (36\text{-}24)$$

† We drop the subscript 21 from p, since we are now considering only one function p.

P will be a function of the upper limit of the triangle (here 1), of x and of V: $P(1, x, V)$. The denominator in (36-24) is the change in V that would occur if the domains behaved independently; we call it $V^0(1, x)$. Hence

$$V\begin{pmatrix} 1 \\ 0 \quad x \end{pmatrix} = V(0,1) - P(1, x, V)V^0(x, 1) \tag{36-25}$$

P is thus the factor by which the potential contribution V^0, which would be observed in the absence of domain interactions, is reduced by this interaction. It is important to note that P depends on the current values of x and of V; the averaging over the triangle has to be done at the end of the path under consideration.

Consider now a primary ascending path. At the reversal point x_l

$$\begin{aligned} V\begin{pmatrix} 1 \\ 0 \quad x_l \end{pmatrix} &= V(0, 1) - P(1, x_l, V_l)\, V^0(x_l, 1) \\ &= V(0, 1) - V(x_l, 1) \end{aligned} \tag{36-26}$$

As x increases again, only those regions in the triangle FIH (Fig. 36-41) which had emptied at x_l will refill. These will amount to a volume $P(x, x_l, V_l)$ $V^0(x_l, x)$, so that

$$V\begin{pmatrix} 1 \quad x \\ 0 \quad x_l \end{pmatrix} = V(0, 1) - V(x_l, 1) + P(x, x_l, V_l)V^0(x_l, x) \tag{36-27}$$

We note in particular that for this ascending process *P depends on the value of V at the reversal point.*

Similarly, for a primary descending curve from the ascending boundary curve

$$V\begin{pmatrix} x_u \\ 0 \quad x \end{pmatrix} = V(0, x_u) - P(x_u, x, V)\, V^0(x, x_u) \tag{36-28}$$

Here *P depends on the current value of V.* The ascending curve resulting from a reversal along this curve at x_l will be given by

$$\begin{aligned} V\begin{pmatrix} x_u \quad x \\ 0 \quad x_l \end{pmatrix} &= V(0, x_u) - P(x_u, x_l, V_l)\, V^0(x_l, x_u) \\ &\quad + P(x, x_l, V_l)\, V^0(x_l, x) \end{aligned} \tag{36-29}$$

These equations can now be employed for developing methods of studying, for a given pair of values of x_l and x_u, the way in which P depends upon V_l.

Consider first a primary ascending (′) and a primary descending (″) scanning curve (Fig. 36-42). Along the ascending curve the increase in V between x_l and x_u will be

$$V'_a(x_l, x_u) = P(x_u, x_l, V'_l)V^0(x_l, x_u) \tag{36-30a}$$

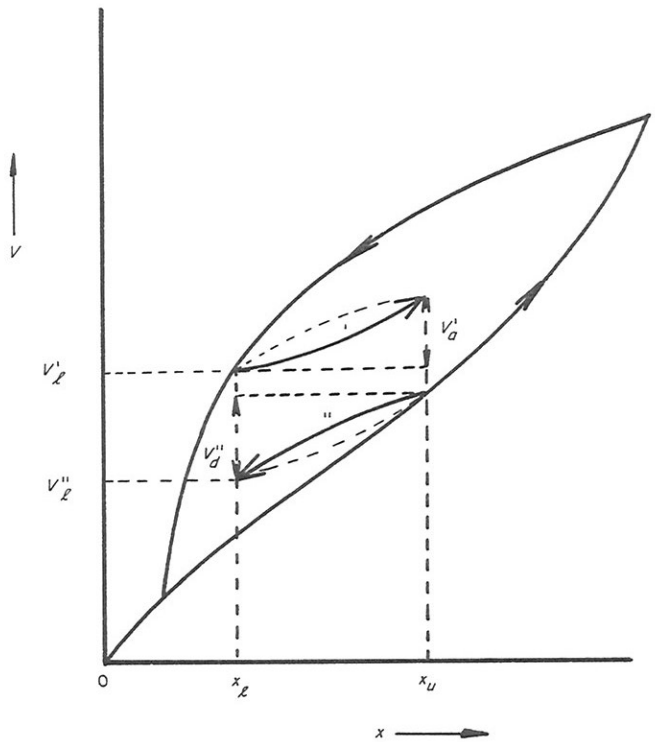

FIG. 36-42. Choice of curves for calculation of relative pore-blocking at different degrees of filling.

while along the descending curve the decrease in V'' between x_u and x_l will be:

$$V''_a(x_u, x_l) = P(x_u, x_l, V''_l)V^0(x_l, x_u) \tag{36-30b}$$

Thus,

$$\frac{P(x_u, x_l, V'_l)}{P(x_u, x_l, V''_l)} = \frac{V'_a}{V''_a} \tag{36-31}$$

We can thus find, for a given pair of values of x_l and x_u, the relative values of P for different values of V. From a complete set of ascending and descending scanning curves we obtain a series of values of $P(V')/P(V'')$. It is not possible to obtain the absolute values of P unambiguously, but by choosing one value arbitrarily we can derive a set of values of P relative to this reference value and examine their dependence on V. An analysis of the data for xenon adsorbed on porous glass (*28,13*) reveals that for this system, at least, all values of P,

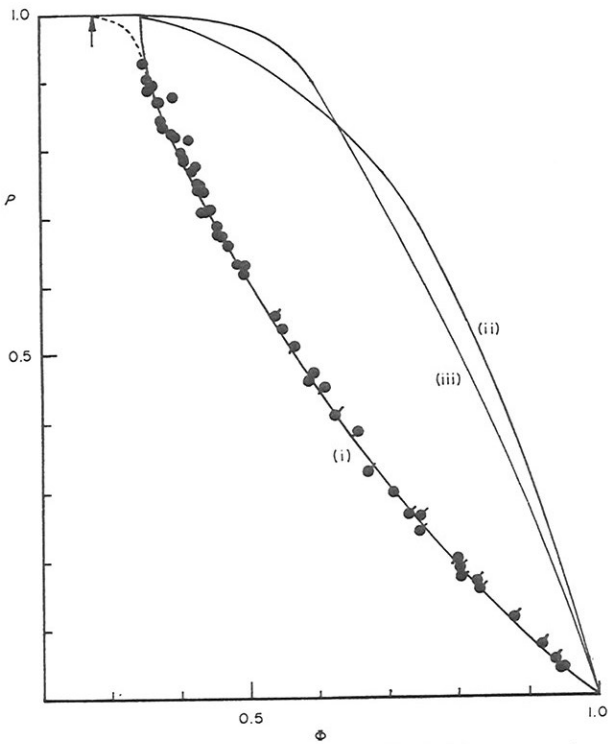

FIG. 36-43. P as function of $V/V^s = \phi$ for xenon adsorbed by porous glass. (i) Experimental: ● from primary scanning curves (*13*), ◐ from internal loops (*13*), ◑ from internal loops (*28*). (ii) Calculated from Ksenzhek (*61*). (iii) Based on random-number calculation of penetration into plane lattice. [Data of (*13*,*28*).]

when plotted against V, lie on the same line, independent of the values of x_l and x_u. This is shown in Fig. 36-43, in which the values of P have been adjusted so that P rises to approximately unity as V decreases, and V has been expressed as the fractional filling V/V^s, denoted by ϕ. Additional values of P can also be obtained by considering the vertical span of internal loops between the same limits x_l and x_u but at different heights in the main loop (dotted in Fig. 36-42); cf. Fig. 36-16. The vertical span is in each case given by a formula of the type (36-30), so that again relative values of P can be calculated. These values are also included in Fig. 36-43. Finally, we may analyze, not only the main boundary curves and the primary scanning curves, but also the scanning curves within subsidiary loops. This has not yet been carried out.

More experimental data are clearly desirable, but the conclusion at this stage appears to be that the pore-blocking mechanism is controlled by the total amount of material condensed in the pore space and is independent of the way in which this liquid is distributed.

Although the importance of pore-blocking in determining the shape of adsorption hysteresis curves has been appreciated previously (*58*,*60*), there has been until now no method of studying the phenomenon quantitatively nor data to which any method could be applied. On the other hand, there have been a number of attempts to predict the effect theoretically (*61*). The only one of these theories which is expressed in a form that can be compared easily with the results shown in Fig. 36-43 is that of Ksenzhek (*61*): the curve deduced from his equations is shown as curve (ii) in Fig. 36-43. A simple model that illustrates the way in which blocking may occur is obtained by considering a random-number table (e.g., of digits) and assuming that it can be entered from one side only by steps following numbers larger than or equal to a chosen number. The area of the table accessible through numbers 9, 8, 7, etc., can then be determined and corresponds to the pores that can be emptied at a given stage in the desorption process. The number of places actually accessible divided by the number potentially accessible is analogous to P, and the fraction of the total number of places that remain actually inaccessible corresponds to ϕ. In a typical calculation of penetration into an array of 5000 random numbers in the range 0 to 99 it was found that, whereas all numbers greater than 60 should give access to 40% of all the sites, only one half of those potentially accessible could in fact be reached. Curve (iii) of Fig. 36-43 shows the results of calculations based on this model; they are in general agreement with Ksenzhek's calculations, which followed a different method and refer to a three-dimensional lattice. The two theoretical curves based on the assumption that the pore properties are distributed in a completely random manner are, however, in complete disagreement with the experimental curve. A possible explanation of this is that the distribution of pore dimensions in porous glass is not random; indeed, it is to be expected that there will be some correlation between the sizes of adjacent pore openings. Before drawing more detailed conclusions, however, it is necessary to establish whether curve (i) is typical of a wide range of porous materials or is peculiar to porous glass. A close study of the form of the curves for pore-blocking for different porous bodies may well give important new information about their structure.

Although it is not the purpose of this chapter to deal with the question of the derivation of pore-size distribution curves from adsorption data, it is important to draw attention to the implications of the pore-blocking phenomenon. If this is ignored, the pore-size distribution curves derived in the conventional manner will be seriously distorted [cf. (*58*)]. The most convenient way of incorporating this correction has, however, yet to be worked out.

36-6. SUMMARY

In this chapter it has not been possible to discuss in detail more than a few aspects of adsorption hysteresis or to present more than a selection of the published experimental work. It is hoped, however, that the examples quoted are representative and include all the major phenomena that have been observed. Emphasis has, indeed, been placed on the wide range of phenomena associated with adsorption hysteresis, and an attempt has been made to show the basic relationships between them through a consideration of the general thermodynamic description of irreversible domain processes. Further unification of the problem is attempted by summarizing the general behavior to be expected from a statistical assembly of domain processes and comparing these predictions with experimental observations.

Little has been said about the overall thermodynamic behavior of statistical assemblies of domains: the theoretical basis of such a discussion is still not firmly established [cf. (62)], and there have been few experimental studies of a precision adequate for testing any theory. The very careful calorimetric study of Kington and Smith (*63*), for example, seems to be inadequate for testing (36-7).

The problems facing a general thermodynamic theory of hysteresis are considerable. There is little doubt that the theories of Brillouin (*5*) and of Duhem (*6*) are erroneous, and it is also doubtful whether the assumptions involved in Bridgman's discussion (*64*) can be justified. The difficulties are brought out in the work of Stoner and Rhodes (*65*) and of Stoner (*66*) on magnetic hysteresis and are summarized for the adsorption case by Hill (*67*).

Nevertheless, despite the problems of establishing an all-embracing thermodynamic theory the limited theoretical ideas summarized in this review focus attention on a range of problems that are capable of more detailed experimental study. Their solution will form the basis of further developments in our understanding of the complex factors controlling adsorption hysteresis.

REFERENCES

1. A. Ewing, *Proc. Roy. Soc.* (*London*), **33,** 22 (1881); **36,** 117 (1883); *Phil. Trans. Roy. Soc.* (*London*), **1885,** 523; *Magnetic Induction in Iron and Other Metals*, London, 1892. The term hysteresis was introduced by Ewing and is derived from the Greek ὑστερέω—"to lag behind."
2. See, e.g., T. Alfrey and P. Doty, *J. Appl. Phys.*, **16,** 700 (1945); D. ter Haar, *Physica*, **16,** 719, 738, 839 (1950).
3. D. H. Everett, *Trans. Faraday Soc.*, **50,** 1077 (1954).
4. J. M. van Bemmelen, *Z. Anorg. Allgem. Chem.*, **13,** 233 (1897).
5. M. Brillouin, *Compt. Rend.*, **106,** 416, 482, 537, 589 (1888); *J. Phys.* **8,** 169 (1889).
6. P. Duhem, *Mémoires l'Acad. Belg. en 4°*, Mém. I, II, III, **54** (1896); Mém. IV, V, **56** (1896); Mém, VI, **62** (1902). Translations of these papers, in some cases in a revised form, and with some additional material, appeared as follows: *Z. Physik. Chem.* (*Leipzig*), **22,** 545 (1897); **23,** 193, 497 (1897); **28,** 577 (1899); **33,** 644 (1900); **34,** 312 (1900); **35,** 91 (1901); **43,** 695 (1903).
7. R. Zsigmondy, *Z. Anorg. Allgem. Chem.*, **71,** 356 (1911).
8. J. S. Anderson, *Z. Physik. Chem.* (*Leipzig*), **88,** 212 (1914).
9. B. Lambert and A. M. Clark, *Proc. Roy. Soc.* (*London*), **A122,** 497 (1929); B. Lambert and A. G. Foster, *ibid.*, **134,** 246 (1931); **136,** 363 (1932); A. G. Foster, *ibid.*, **147,** 128 (1934); **150,** 77 (1935).
10. L. H. Cohan, *J. Am. Chem. Soc.*, **66,** 98 (1944).
11. Summarized by J. C. Arnell and H. L. McDermott, in *Surface Activity*, Vol. 2 (J. H. Schulman, ed.), Butterworth, London, 1957, p. 113.
12. J. H. de Boer, in *Structure and Properties of Porous Materials* (D. H. Everett and F. S. Stone, eds.), Butterworth, Colston Papers, Vol. 10, London, 1958, p. 68.
13. A. J. Brown, Ph.D. thesis, Bristol, 1963.
14. H. E. Riess, in *Advances in Catalysis*, Vol. 4 (W. G. Frankenburg, V. I. Komarewsky, and E. K. Rideal, eds.), Academic, New York, 1952, p. 87.
15. (a) D. A. Cadenhead, Ph.D. thesis, Bristol, 1957; (b) D. A. Cadenhead and D. H. Everett, *Industrial Carbon and Graphite*, Soc. Chem. Ind., London, 1958, p. 272.
16. R. M. Barrer and J. S. S. Reay, in *Surface Activity*, Vol. 2 (J. H. Schulman, ed.), Butterworth, London, 1957, p. 79.
17. A. R. Urquhart and A. Williams, *J. Textile Inst.*, **15,** T146, (1924).
18. J. M. Holmes and R. A. Beebe, *J. Phys. Chem.*, **61,** 1684 (1957).
19. A. Bailey, Ph.D. thesis, Bristol, 1965.
20. R. M. Barrer and K. E. Kelsey, *Trans. Faraday Soc.*, **57,** 452 (1961).
21. A. M. Kinnear, Ph.D. thesis, St. Andrews, 1953; D. A. Cadenhead, Ph.D. thesis, Bristol, 1957.
22. J. Renon, J. Francois-Rossetti, and B. Imelik, *Bull. Soc. Chim. France*, **1960,** 446.
23. H. Van Olphen, *J. Colloid Sci.*, **20,** 822 (1965).
24. C. H. Amberg, D. H. Everett, L. Ruiter, and F. W. Smith, in *Surface Activity*, Vol. 2 (J. H. Schulman, ed.), Butterworth, London, 1957, p. 3.
25. A. J. Miles, Ph.D. thesis, Bristol, 1964; A. Bailey, Ph.D. thesis, Bristol, 1965.
26. M. M. Dubinin, B. P. Bering, V. V. Serpinsky, and B. N. Vasilev, *Surface Phenomena in Chemistry and Biology* (J. F. Danielli, K. G. A. Pankhurst, and A. C. Riddiford, eds.), Pergamon, New York, 1958, p. 172.
27. K. S. Rao, *J. Phys. Chem.*, **45,** 500, 506, 513, 517 (1941); P. H. Emmett and M. Cines, *J. Phys. Chem.*, **51,** 1255 (1947); H. W. Quinn and R. McIntosh, in *Surface Activity*, Vol. 2 (J. H. Schulman, ed.), Butterworth, London, 1957, p. 122; *Can. J. Chem.*, **35,** 745 (1957).
28. N. J. Blakeney-Edwards, Ph.D. thesis, Bristol, 1963; cf. A. J. Brown, Ph.D. thesis, Bristol, 1963.
29. D. H. Everett and W. I. Whitton, *Proc. Roy. Soc.* (*London*), **A230,** 91 (1955).
30. H. Barkhausen, *Phys. Z.*, **20,** 401 (1919).
31. (a) D. H. Everett and W. I. Whitton, *Trans. Faraday Soc.*, **48,** 749 (1952); (b) D. H. Everett and F. W. Smith, *ibid.*, **50,** 187 (1954); (c) D. H. Everett, *ibid.*, **50,** 1077 (1954); **51,** 1551 (1955); (d) J. A. Enderby, *ibid.*, **51,** 835 (1955); **52,** 106 (1956).
32. See, e.g., I. Prigogine and R. Defay, *Chemical Thermodynamics* (transl. D. H. Everett), Wiley (Interscience), New York, 1954.
33. D. H. Everett and P. Norden, *Proc. Roy. Soc.* (*London*), **A259,** 341 (1960).
34. I. Higuti, *Sci. Rep. Tohoku Univ. First Ser.*, **37,** 142 (1953).
35. T. L. Hill, *J. Chem. Phys.*, **15,** 767 (1947).

36. W. Thomson, *Phil. Mag.*, **42,** 448 (1871).
37. W. A. Patrick, *Coll. Symp. Ann.*, **7,** 129 (1930).
38. K. S. Rao, *J. Phys. Chem.*, **45,** 500, 506, 513, 517 (1941).
39. See, e.g., *Contact Angle, Wettability and Adhesion, Advances in Chemistry Series No. 43,* American Chemical Society, Washington, D.C., 1964.
40. A. G. Foster, *Trans. Faraday Soc.*, **28,** 645 (1932).
41. E. O. Kraemer, in *Treatise on Physical Chemistry* (H. S. Taylor, ed.), Van Nostrand, New York, 1931, p. 1661.
42. J. W. McBain, *J. Am. Chem. Soc.*, **57,** 699 (1935).
43. R. M. Barrer, N. McKenzie, and J. S. S. Reay, *J. Colloid. Sci.*, **11,** 479 (1956).
44. Cf. Lord Kelvin, *Scientific Papers*, Vol. II, p. 574; C. V. Boys, *Soap Bubbles*, Science Study Series, Heineman, London, 1960.
45. J. M. Haynes, Ph.D. thesis, Bristol, 1965.
46. S. Brunauer, *Physical Adsorption of Gases and Vapours*, Oxford, New York, 1943, p. 394.
47. S. M. Katz, *J. Phys. Chem.*, **53,** 1166 (1949).
48. Representative recent papers which contain references to earlier work are: I. Higuti and H. Utsugi, *J. Chem. Phys.*, **20,** 1180 (1952); B. G. Aristov, A. P. Kharnaukhov, and A. V. Kiselev, *Russ. J. Phys. Chem.* (*English transl.*), **36,** 1159 (1962); R. Venable and W. H. Wade, *J. Phys. Chem.*, **69,** 1395 (1965); J. C. Melrose, *Soc. Petrol. Engrs. J.*, **5,** 259 (1965).
49. D. H. Everett, in *Structure and Properties of Porous Materials* (D. H. Everett and F. S. Stone, eds.), Butterworth, Colston Papers, Vol. 10. London, 1958, p. 95.
50. Cf. D. H. Everett and W. I. Whitton, *Trans. Faraday Soc.*, **48,** 749 (1952); J. C. Melrose has also drawn attention to this aspect of the problem, private communication, 1965, and see *A. I. Ch. E. J.*, **12,** 986 (1966).
51. See, e.g., H. N. V. Temperley, *Proc. Phys. Soc.* (*London*), **59,** 199 (1947); other papers dealing with the ultimate tensile strength of liquids are: S. W. Benson and E. Gerjuoy, *J. Chem. Phys.*, **17,** 914 (1949); **18,** 215 (1950).
52. G. A. Saunders, A. R. Ubbelohde, and D. A. Young, *Proc. Roy. Soc.* (*London*), **A271,** 499 (1963).
53. Cf. E. Hückel, *Adsorption und Kapillarkondensation*, Akademische Verlagsgesellschaft, Liepzig, 1928, p. 272.
54. M. B. Coelingh, *Kolloid-Z.*, **87,** 251 (1939).
55. P. C. Carman and F. A. Raal, *Nature*, **167,** 112 (1951); *Proc. Roy. Soc.* (*London*), **A209,** 59 (1951).
56. P. C. Carman, *J. Phys. Chem.*, **57,** 56 (1953).
57. P. H. Emmett and M. R. Cines, *J. Phys. Chem.*, **51,** 1255 (1947).
58. H. W. Quinn and R. McIntosh, in *Surface Activity*, Vol. 2 (J. H. Schulman, ed.), Butterworth, London, 1957, p. 122; *Can. J. Chem.*, **35,** 745 (1957).
59. N. Collis-George, *Proc. Natl. Acad. Sci.* (*India*), **24A,** 80 (1955); Youngs, E. G., *Trans. Internat. Cong. Soil Sci. 7th*, **1,** 107 (1960); A. Poulovassilis, *Soil Sci.*, **93,** 405 (1962); J. R. Philip, *J. Geophys. Res.*, **69,** 1553 (1964).
60. D. H. Everett, in *The Structure and Properties of Porous Materials* (D. H. Everett and F. S. Stone, eds.), Butterworth, Colston Papers, Vol. 10, London 1958, p. 116; J. A. Barker, *ibid.*, p. 125.
61. See, e.g., I. Fatt, *Trans. AIME*, **207,** 144 (1956); C. G. Dodd and O. G. Kiel, *J. Phys. Chem.*, **63,** 1646 (1959); H. L. Frisch, J. H. Hammersley, and D. J. A. Welsh, *Phys. Rev.*, **126,** 949 (1962); O. S. Ksenzhek, *Russ. J. Phys. Chem.* (*English transl.*), **37,** 691 (1963); C. C. Harris, *Nature*, **205,** 353 (1965).

62. D. H. Everett and W. I. Whitton, *Proc. Roy. Soc.* (*London*), **A230,** 91 (1955).
63. G. L. Kington and F. S. Smith, *Trans. Faraday Soc.*, **60,** 705, 721 (1964).
64. P. W. Bridgman, *Rev. Mod. Phys.*, **22,** 56 (1950).
65. E. C. Stoner and P. Rhodes, *Phil. Mag.*, **40,** 481 (1949).
66. E. C. Stoner, *Rev. Mod. Phys.*, **25,** 2 (1953).
67. T. L. Hill, *J. Chem. Phys.*, **17,** 520 (1949).